UNIVERSITÀ DEGLI STUDI DI PADOVA

DIPARTIMENTO DI INGEGNERIA DELL'INFORMAZIONE

DIPARTIMENTO DI INGEGNERIA DELL'INFORMAZIONE

CORSO DI LAUREA MAGISTRALE IN BIOINGEGNERIA INDUSTRIALE

3D BIOPRINTING FOR THE PRODUCTION OF CELL-LADEN VASCULARIZED CONSTRUCTS

RELATORE:
Prof.ssa Elisa Cimetta

CORRELATORE:
Dott. Federico Maggiotto

LAUREANDA:
Camilla Pozzer
Matricola 2020563

ANNO ACCADEMICO 2021-2022

DATA DI LAUREA 5/10/2022

S A T O R
A R E P O
T E N E T
O P E R A
R O T A R

Riassunto

Lo sviluppo delle conoscenze della biologia cellulare integrate con quelle della bioingegneria ha aperto il campo all'ingegneria tissutale, che propone l'utilizzo di cellule e materiali per la formazione in laboratorio di costrutti utili alla ricerca, allo studio e allo sviluppo di modelli atti ad investigare malattie e, di conseguenza, terapie mirate. Per più di un secolo la cultura cellulare bidimensionale (2D) è stata utilizzata come modello *in vitro* per lo studio della risposta cellulare. Lo sviluppo tecnologico ha però evidenziato come tale modello porti a risultati significativamente differenti dalla realtà dei modelli *in vivo*, in particolar modo nello studio di cellule tumorali. Per far fronte ai limiti caratteristici del modello bidimensionale, le ricerche recenti hanno spostato l'attenzione a strutture tridimensionali (3D) in grado di ricreare un ambiente biomeccanico e biochimico più realistico [1]. Lo scopo di questa tesi è infatti quello di creare un modello tridimensionale di tessuto vascolarizzato tumorale, concentrandosi particolarmente nella realizzazione *in vitro*, tramite l'utilizzo di biostampa 3D sacrificale, di un canale endotelializzato perfondibile.

Malgrado i vantaggi rappresentati dalle culture tridimensionali, restano evidenti alcune sfide che riguardano lo spessore dei costrutti, la meccanica del microambiente e la distribuzione spaziotemporale di ossigeno, nutrienti e rifiuti metabolici. Più spesso è il costrutto, infatti, più difficile sarà per le cellule ricevere i nutrienti necessari al loro corretto funzionamento. Da qui la necessità di creare una vascolarizzazione nel costrutto, al fine di poter trasportare in modo efficiente il mezzo di coltura cellulare attraverso la struttura, simulando così il comportamento di una rete vascolare.

La struttura tridimensionale finale sarà quindi frutto dell'interazione tra le linee cellulari e il materiale impiegato per il processo di stampa. Ecco che la scelta del materiale è un passaggio fondamentale nello sviluppo della ricerca. I materiali maggiormente utilizzati sono gli hydrogel, grazie alla loro capacità di mimare le proprietà meccaniche della matrice extracellulare dei tessuti, garantendo a fattori solubili di viaggiare nel costrutto. Per questa tesi si è scelto di utilizzare due diversi tipi di hydrogel. Il primo, che contiene e raccoglie le cellule, è la gelatina metacrilata (GelMA). La GelMA è stata scelta grazie alle caratteristiche di elevata biocompatibilità, biodegradabilità e termoreversibilità che ne consente la

biostampa in condizioni ambientali e la successiva reticolazione quando sottoposta a radiazioni UV.

Per realizzare il canale vascolare si utilizza il Pluronic® F-127. Sfruttando la sua caratteristica di termoreversibilità, una volta terminata la stampa tale materiale viene eliminato dalla struttura, creando così uno spazio vuoto all'interno della matrice. Tale canale verrà quindi rivestito da tessuto endoteliale ed utilizzato per il trasporto dei nutrienti alle cellule che compongono lo scaffold.

Con lo scopo di ricreare il tessuto endoteliale sono state scelte linee cellulari derivate dalla vena del cordone ombelicale (HUVECs) e staminali mesenchimali derivate dal midollo osseo (MSCs).

Summary

Advancements in knowledge of cell biology integrated with that of bioengineering has opened the field to tissue engineering, which proposes the use of cells and materials to form constructs in the laboratory that are useful for research, study, and development of models suitable for investigating diseases and, ultimately, developing targeted therapies. For over a century, two-dimensional (2D) cell culture has been used as an *in vitro* model for the study of cellular response. However, technological development has shown that this leads to results differing from the reality of *in vivo* systems, especially in the study of cancer cells. To address the characteristic limitations of the two-dimensions, recent research has shifted the focus to three-dimensional (3D) structures capable of recreating a more realistic biomechanical and biochemical environment [1]. With this in mind, the purpose of this thesis is to create a three-dimensional model of vascularized tumor tissue, focusing on the *in vitro* fabrication through the use of sacrificial 3D bioprinting and endothelialization of a perfusable channel.

Despite the advantages represented by 3D cultures, some challenges remain evident involving construct thickness, microenvironment mechanics, and spatiotemporal distribution of oxygen, nutrients, and metabolic wastes. The thicker the construct, the more difficult it will be for the cells to receive the nutrients necessary for their proper functioning. Hence the need to create a vasculature in the construct to efficiently transport cell culture medium through the structure, simulating the behavior of the *in vivo* vascular network.

The final three-dimensional structure will then result from the interaction between the cell lines and the material used for the printing process. Here the choice of material is a key step in research development. The most used materials are hydrogels, due to their ability to mimic the mechanical properties of the extracellular matrix of tissues, ensuring soluble factors transport into the construct. Two different hydrogels were chosen for this thesis. The first, which serves as a cell 3D support, is gelatin methacrylate (GelMA). GelMA was chosen because of its characteristics of high biocompatibility, biodegradability and thermoreversibility, which allows it to be bioprinted under standard laboratory conditions and then cross-linked when subjected to UV radiation.

Pluronic® F-127 is used to fabricate the vascular channel. Taking advantage of its thermoreversibility, once printing is finished such material is removed from the structure, thus creating an empty space within the matrix. This channel will then be lined with endothelial cells and used to transport nutrients to the cells in the bulk of the scaffold.

With the aim of recreating the endothelial tissue, umbilical vein-derived endothelial cells (HUVECs) and bone marrow-derived mesenchymal stem cells (MSCs) were used.

CONTENTS

LIST OF FIGURES

LIST OF TABLES

INTRODUCTION

For many years, the study of cellular response has focused on the *in vitro* use of two-dimensional (2D) cultures. Recent technological developments have shown how these models diverge from reality, so the focus has shifted to three-dimensional (3D) constructs that can recreate a more physiologically realistic environment. Next to the many advantages that this brings, there are a few disadvantages, the main one being the fact that the thickness of the constructs prevents proper nutrient transport to the cells in the bulk. Hence the need to create a vascularized construct, which development requires several skills from the materials choice to the proper structure design. The best choice for materials is hydrogels: polymeric or natural materials that are biocompatible, biodegradable, and nontoxic, making them excellent for use in the biological field to mimic the mechanical properties of tissues.

Several techniques can be used to achieve this purpose, and in this thesis we chose to focus on 3D bioprinting. The experiments were performed at the BIAMET laboratory (*Biomedical Applications of Multiscale Engineering Technologies*) in collaboration with *Istituto di ricerca pediatrica – Città della speranza* (IRP) in Padova. The goal is to make a fully endothelialized channel that can be perfused and mimics the behavior of a blood vessel, to perform studies on Neuroblastoma, a childhood solid tumor originating from progenitor cells of the sympathetic nervous system.

The work done is divided into four main chapters listed below.

The first one provides an overview of the background, briefly introducing the concept of mechanotransduction, 2D and 3D cultures (focusing on the advantages of the latter), the main 3D bioprinting methods, and the materials and techniques chosen to produce the structure.

The second chapter summarizes the procedures and protocols followed for materials synthesis and the bioprinting process. Special attention is given to the design of the chosen structure and of the clamp unit created to ensure sterility and stability for the entire duration of the experiment. The last part of this chapter contains the protocols used for biological validation and image acquisition.

The third chapter presents the main and most promising results obtained in this thesis, starting from the bioprinting and circuit setup, and concluding with the cellular tests.

The final chapter summarizes all the steps that led to the obtained results, and general conclusions about the methods applied are drawn. Improvements and alternatives on the explained experiments are suggested for the continuation and development of future projects.

For completeness, the Appendix contains additional information on material synthesis and more complete protocols for the endothelialization and immunofluorescence steps.

Chapter 1
STATE OF THE ART

In this chapter, some fundamental concepts will be introduced to better understand the developed thesis project. Topics include an explanation of the concept of cell cultures, with attention to the difference between 2D and 3D environments and a hint to the main techniques for 3D bioprinting. The printing materials used for cell growth and adhesion will also be presented, with a focus on those used in this thesis project. Finally, possible uses of these materials will be presented, mainly referring to the main purpose of the project.

1.1 CELL ENVIRONMENT

Physicochemical features of the environment exert important influence on cell behavior and include the influence of matrix elasticity and topography on differentiation processes. The presence of protein and growth factors on these matrices provides chemical cues and thus plays vital role in directing cell fate. Engineering of functional biomimetic scaffolds that present spatio-temporal physical and chemical signals to cells holds great promise in tissue engineering and in cell therapy. Progress in this field requires deep understanding of the mechanistic aspects of cell-environment interactions, so that they can be manipulated and exploited for the design of sophisticated biomaterials [2].

1.1.1 INFLUENCE OF ECM ON CELL BEHAVIOUR

In all tissues, cells live in contact with a specific milieu called extracellular matrix (ECM). Since the early developmental phases, embryonic cells produce their own extracellular matrices, by secreting many types of molecules in the surrounding space, according to a well-defined program of differentiation. Understanding cell differentiation and function means understanding the environment in which cells are contained and the mechanisms of cell-cell and cell-extracellular matrix (ECM) communication [3].

The ECM is a composite of cell-secreted molecules that offers biochemical and structural support to cells, tissues, and organs. In humans, the composition of the

ECM can be broadly summarized as a combination of water, proteins, and polysaccharides, with the precise balance of these three compartments reflecting functional specificities of each tissue. The structural requirements determine the mechanical properties of the ECM, which depend on the protein composition of the matrix, particularly the abundance of collagen and elastin. The physiological relevance of these properties extends beyond simple structural integrity. The cells surrounded by the ECM can sense its rigidity through integrin-mediated interactions with the matrix. The mechanical properties of the matrix are then interpreted and affect motility, proliferation, differentiation, and apoptosis [4].

The molecular organization and function of these interactions are adaptive and vary between cell types and tissues. Although commonly studied as separate biophysical domains, the functions of the ECM and cells are strictly interdependent and coevolve in all tissues. The resulting crosstalk results in a gradual evolution of both the cell and the tissue through which it migrates. Cells and engaged tissues can be regarded as multi-component viscoelastic units, subject to reciprocal mechanochemical interactions that induce, guide or limit cell migration in a context-dependent manner [5]. During migration, cells generate active pulling forces via actin filaments contraction; these forces are then transmitted to the ECM fibers through focal adhesion complexes and result in ECM's remodeling and can also be sensed by other cells in the system. In multicellular systems, the pulling forces generated by individual cells can give rise to a dynamically evolving network: forces propagate in the ECM, influence the migration of the individual cells, which in turn alter the ECM structure and properties [6].

The relationships between the cell and its ECM context are inherently bi-directional, and aptly described by the term 'mechanoreciprocity' [5]. The ability of cells to sense and respond to mechanical stimuli is termed mechanotransduction. This requires the sensing of external forces and the transduction of this information, triggering a specific intracellular signaling response. Sensing of the mechanical environment enables cells to rapidly respond to whole tissue parameters such as ECM stiffness, influencing decisions regarding the form, function, and fate of the cells [7].

1.1.2 2D AND 3D CELL CULTURE

Cell culture is an indispensable tool to help uncover fundamental biophysical and biomolecular mechanisms by which cells assemble into tissues and organs, how tissues function, and how function becomes disrupted in disease. Cell cultures *in vitro* are frequently used to advance understanding of the mechanisms that underlie cell behavior *in vivo*. These behaviors include cell differentiation, migration, growth, and mechanics, all of which are impacted by their biochemical and biomechanical microenvironment. Decades of fundamental research have strictly relied on flat, two-dimensional (2D) cell cultures, but more recent research has shifted towards the use of three-dimensional (3D) structures [1]. Some key differences between 2D and 3D cultures will be presented below, useful to understand the importance of research and the necessary future developments.

Conventional adherent tissue culture involves growing cells on solid flat surfaces as 2D monolayers. Cells are adhering to a plastic or glass substrate and are in contact with other cells only at their periphery. The cells are not allowed to pile on top of one another, so the 2D surface inhibits the capacity for cells to form a multi-dimensional structure [8].

Although 3D culture systems provide a model that better mimics cell–cell interactions and cell–ECM interactions, compared to the traditional 2D monolayer, and provide an opportunity for co-culture of different type of cells, the current 3D systems still lack the complex vascular systems that support tissues *in vivo* for oxygenation, nutrients transport, and waste removal. Cells grown in 3D culture perform these functions relying on the sole diffusion, and the insufficient availability of growth factors and metabolites influences cell proliferation rate, which is reduced in 3D [9].

Another important difference between 3D and 2D culture concerns the morphology of cells. The non-physiological morphology of 2D cells can affect their function, internal structural organization, secretion, and cell signaling, with a strong impact in pH variation, binding efficacy and altered response to pharmaceutical agents [10]. Furthermore, due to disturbances in the interactions with the external environment, adherent growing cells lose their polarity, which changes their response to various phenomena such as apoptosis. In 3D cultures, the morphology and polarity of cells are maintained, and the similarity to the *in vivo* environment in terms of topology, gene expression, and signaling is better replicated [10]. Cells

cultured in 3D systems receive signals not only at their ventral surface but in all dimensions [12]. A final important consideration addresses the mechanical response of cells: when cultured in 2D, cells only move along a flat surface generating enough traction to overcome its inhibition, while when in 3D they experience inhibition from potential surface contact, from other cells and from the ECM [1]. The main differences between 2D and 3D microenvironments are summarized in Figure 1.1.

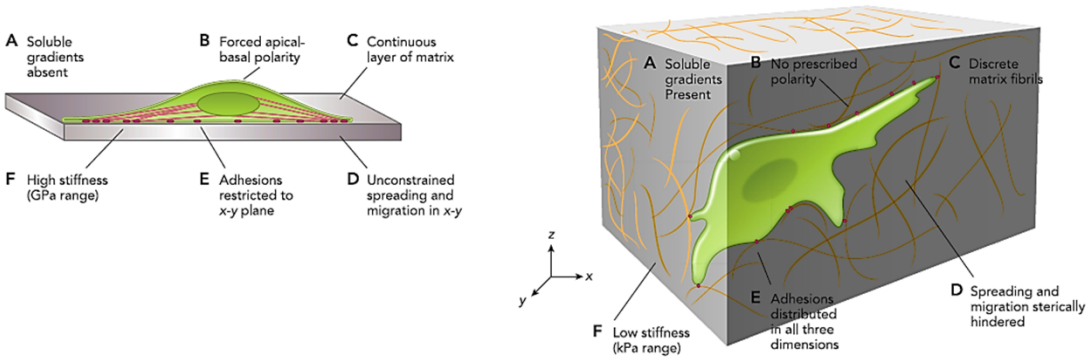

Figure 1.1*: main differences between cells in 2D and 3D microenvironments [1].*

1.2 3D BIOPRINTING

3D bioprinting, or simply bioprinting, is the process that involves patterning and assembly of living and non-living biomaterials via a 3D structural organization using computer-aided transfer processes [13]. Further assisted with computer aided design (CAD) technologies, bioprinting can produce complex 3D structures from the nanoscale to the microscale, efficiently and economically. A tissue or organ blueprint is formed by computer aided design in pre-processing stage and the detailed information of the printed structure in 3D should be determined. The crucial information of anatomy, histological structure, composition, and human organ topology could be obtained using imaging approaches such as magnetic resonance imaging (MRI) or computer tomography (CT) scan [14].

Biofabrication aims at exploiting automated processes, for the most part Additive Manufacturing (AM) techniques, to generate cell-biomaterial constructs that, through their internal and external spatial arrangement, may mature into functional tissue equivalents [15].

Many traditional 3D printing modalities require conditions potentially lethal to cells such as high temperature, toxic chemicals, or a dry environment. These techniques can be still used to produce scaffolds that will house cells only at a later stage following the printing step, but still maintain limitations including the difficulty controlling cell distribution and concentration. When 3D printing technologies are directly coupled with cells, it is referred to as 3D bioprinting and the materials involved are generally termed bioinks [16]. There are various 3D printing techniques that are currently being used in research or commercial applications, with laser assisted printing, stereolithography, inkjet printing, and extrusion printing as the most widely adopted [14].

1.2.1 LASER ASSISTED BIOPRINTING (LAB)

The origin of laser assisted bioprinting is based on modified laser direct writing and laser induced forward transfer techniques. A laser assisted printing system usually consists of four parts: a pulsed laser source, a laser focusing tool, a laser energy absorbing metallic ribbon film, and a receiving substrate. The ribbon structure contains two layers with the upper energy absorbing layer (glass coated with gold or titanium film). During the printing process, schematized in Figure 1.2, a laser pulse focuses on the upper layer at the designed area with film evaporation. The interface produces a high-pressure bubble at the bottom layer with the suspended bioink that is further ejected onto the receiving substrate in droplets [14]. LAB has many advantages compared to other bioprinting methods, and the main one is the fact that it does not use any nozzle, ensuring LAB processing bioink without clogging problems even if the bioink is very viscous. Moreover, LAB can deposit the material with high accuracy and printing resolution (the resolution can reach the micron level) and can cooperate with other bioprinting technologies to extend its capability. Although LAB is one of the most promising bioprinting technologies, it also has some weaknesses: limited by the small volume of biomaterials that can be transferred in each laser pulse, the productivity and printing efficiency is still not the highest among all bioprinting methods [17].

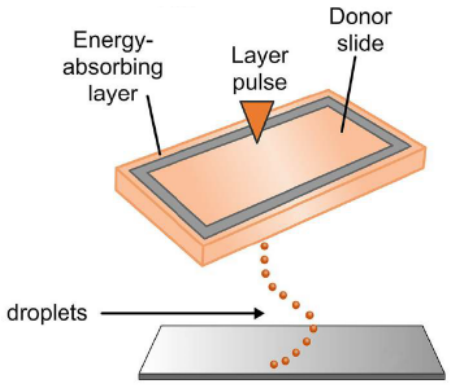

Figure 1.2: *Laser Assisted Bioprinting (LAB) [19].*

1.2.2 STEREOLITHOGRAPHY

Stereolithography relies on spatially controlled illumination to selectively crosslink a liquid bioink into solid hydrogel features [18]. The stereolithography-based bioprinting system, shown in Figure 1.3, uses digital micromirror arrays to control the light intensity of each pixel for printing areas in which light-sensitive polymer materials are polymerized. Stereolithography is a nozzle-free printing technique, which results in an enhanced cell viability, shorter printing time (<1 hr) and high resolution (<100 μm) [19]. While this strategy is exciting and effective, the lack of commercial or open-source hardware, the possible toxicity of photoinitiators and the impossibility of manufacturing multi-material structures has likely slowed adoption by the wider bioprinting community [18].

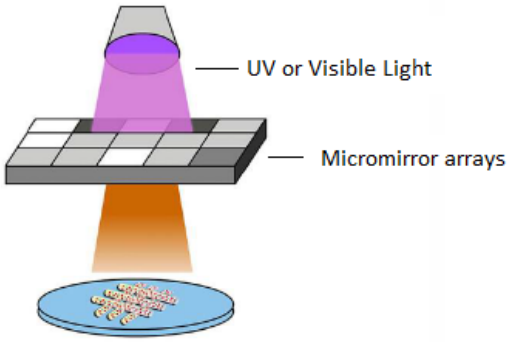

Figure 1.3: *Stereolithography Bioprinting [19].*

1.2.3 INKJET BIOPRINTING

Inkjet bioprinting is a non-contact printing technique that reproduces digital pattern information onto a substrate with small ink drops. There are mainly thermal and piezoelectric approaches to create drops on demand, whose operations are illustrated in Figure 1.4. In thermal inkjet printers, small air bubbles generated by heating in the printhead (up to 300°C) collapse to provide pressure pulses to eject ink drops out of the nozzle. As for the piezoelectric inkjet printers, the actuator of polycrystalline piezoelectric ceramic in each nozzle provides the transient pressure to eject the ink drops onto the substrate [20]. Thermal inkjet bioprinting is an efficient, high speed and economic approach, however, there are still many challenges. The droplet directionality is poor, the required temperature is high, the bioink must be in the liquid phase with low viscosity, and the geometrical shapes are usually irregular. In addition, possible nozzle clogging is frequently affecting the bioprinting process. Although inks in the piezoelectric system are not exposed to heat, the range of frequencies employed can cause cell damage and lysis [14],[21].

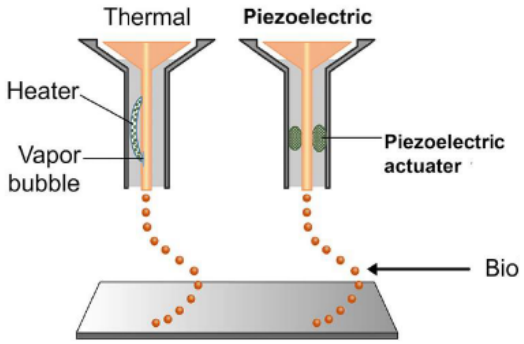

Figure 1.4*: Inkjet Bioprinting [19].*

1.2.4 EXTRUSION BIOPRINTING

Extrusion bioprinting can be seen as a modification of inkjet printing: to print the viscous materials inkjet printers cannot deposit, extrusion bioprinters uses either an air-force pump or a mechanical screw plunger (Figure 1.5). By applying a continuous force, extrusion bioprinting can print uninterrupted cylindrical filaments rather than a single bioink droplet. Almost all types of hydrogel pre-

polymer solutions of varying viscosity, as well as aggregates with high cell density, can be printed using a stage and one or more temperature-controlled cartridges (*i.e.*, syringes or pens). The operator can control the extrusion procedure, speed, and the displacement of the cartridge, and/or the stage in *x*, *y*, and *z* directions, by means of a computer software program [22], [23].

Extrusion is a nozzle-based technique so, as mentioned for inkjet method, there is always a risk of nozzle clogging. Another critical issue in extrusion bioprinters is the loss of cell viability due to shear stress applied to the bioink (materials with encapsulated cells) at a small orifice [21]. Besides this, bioprinting extrusion is the most widely used commercial 3D printing technology due to its acceptable compatibility with different types of materials, good control of shapes, pores, porosity and cellular distribution of printed scaffolds [14].

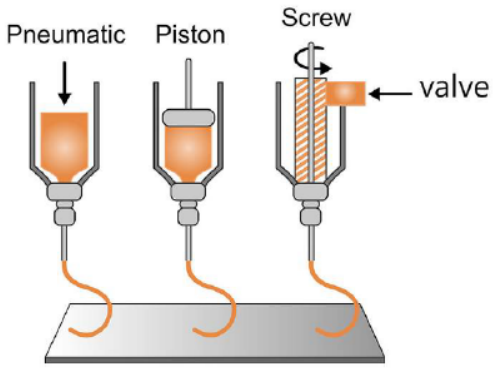

Figure 1.5*: Extrusion Bioprinting [19].*

1.3 HYDROGEL

Hydrogels are networks of polymer chains that are sometimes found as colloidal gels in which water is the dispersion medium. The most common definition is that a hydrogel is a water-swollen and cross-linked polymeric network produced by the simple reaction of one or more monomers. Another definition is that it is a polymeric material that exhibits the ability to swell and retain a significant fraction of water within its structure but will not dissolve in it [24]. The water holding capacity of hydrogels arise mainly due to the presence of hydrophilic groups

(amino, carboxyl and hydroxyl) in the polymer chains. According to research, the amount of water present in a hydrogel may vary from 10-20% to thousands of times of the weight of the xerogel (xerogel is the polymeric network devoid of water). The water holding capacity of a xerogel is dependent on the number of hydrophilic groups and cross-linking density. The higher the number of hydrophilic groups, the higher the water holding capacity, while with an increase in cross-linking density there is a decrease in the equilibrium swelling [25]. Hydrogels are characterized as either synthetic or natural, based on the nature of their constituent polymers. The use of natural hydrogels in the biomedical field is advantageous due to their biocompatibility, biodegradability and non-toxicity, whereas synthetic hydrogels are hydrophobic, possessing strong covalent bonds within their matrix, which improves the mechanical strength, service life and absorbability [26]. Synthetic polymers are more common because they have well-defined structures that can be modified, but the absence of cell-binding motifs in their chains represent a great disadvantage. When extensive functionalization is to be avoided, blending a synthetic polymer with a natural one can offer tunable mechanical and printing properties together with cell-binding sites [24].

1.3.1 CLASSIFICATION OF HYDROGEL

Hydrogel products can be classified on different bases as detailed below [24], [27], [28], [29]:

- Classification based on *source*. As said before, hydrogel can be natural, synthetic or hybrid, based on the properties of the starting polymer.
- Classification according to *preparation method*. There are three different types of hydrogels:
    - Homopolymeric, referred to polymer network derived from a single species of monomer.
    - Copolymeric, comprised of two or more different monomer species with at least one hydrophilic component.
    - Multipolymer Interpenetrating polymeric hydrogel (IPN), made of two independent cross-linked synthetic and/or natural polymer component, contained in a network form.

- Classification according to *network electrical charge*. Hydrogels may be categorized into three groups based on presence or absence of electrical charge located on the cross-linked chains:
    - Nonionic (neutral).
    - Ionic (including anionic or cationic).
    - Amphoteric electrolyte (ampholytic) containing both acidic and basic groups.
- Classification based *on type of cross-linking*. Physical processes such as hydrophobic association, chain aggregation, ionic interaction and hydrogen bonding allow reversible hydrogels due to the conformational changes. On the other hand, chemically cross-linked networks have permanent junctions, so chemical hydrogels are irreversible.
- Classification based on *physical appearance and properties.* The appearance of hydrogels as matrix, film or microspheres depends on the polymerization technique involved in the preparation process. Furthermore, hydrogels are classified into two types based on physical properties. There are conventional hydrogels and smart hydrogels. Smart hydrogel, also called stimuli responsive hydrogels, respond to environmental stimuli (temperature, light, pH, pressure, electric and magnetic fields) and experience changes in their growth actions, network structure, mechanical strength, and permeability.

1.3.2 GELATIN BASED HYDROGEL

Among all hydrogel materials, gelatin has gained extensive attention as a promising and attractive polymer backbone for tissue regeneration. Gelatin has desirable properties, such as the presence of bioactive moieties, biocompatibility, biodegradability, and low antigenicity as well as cost effectiveness. Conventionally, gelatin is extracted from porcine, bovine, or fish skin collagen (mainly type I). Collagen is hydrolyzed to protein fragments by acidic or basic treatment, which produces type A or type B gelatin, respectively. Importantly, gelatin contains bioactive sequences derived from collagen (e.g., RGD peptides and MMP-sensitive degradation sites). Additionally, various functional groups

(e.g., primary amine, carboxyl, and hydroxyl groups) in gelatin enable to be modified with various crosslinkers or therapeutic agents, thus increasing its applicability as a versatile material for wound healing, drug delivery system and tissue engineering [30]. Gelatin is easily soluble in water at 37°C. A typical property of the gelatin solution is the capability to gelate at low temperature (about 20–25°C) to form hydrogels; this process is called sol-gel transition. During the gelation process, locally ordered regions among the gelatin molecules form, that are subsequently joined by non-specific bonds, such as hydrogen, electrostatic and hydrophobic bonds. The resultant hydrogel has a unique thermo-reversible character since the non-specific bonds can be easily broken by heating the polymer [31].

Since at a body temperature of 37°C gelatin is a liquid, it is immediate to say that pure gelatin cannot be used for tissue engineering purposes. This "defect" of gelatin hydrogels is addressed with crosslinking technique. Crosslinking can be performed via several methods including physical crosslinking such as dehydrothermal treatment (DHT), plasma treatment, and ultraviolet (UV) treatment; enzymes crosslinking, such as transglutaminase and horseradish peroxidases, and chemical crosslinking by agents such as glutaraldehyde or carbodiimides. The crosslinking treatment can improve not only the water-resistant ability but also the thermo-mechanical performance of the treated fiber, leading to an enhanced mechanical strength [32].

1.3.3 GELATIN METHACRYLATE (GelMA)

GelMA hydrogels are based on a modified gelatin which is prepared by reaction of gelatin with methacrylic anhydride (MA) [34]. The introduction of methacryloyl substituent groups, as shown in Figure 1.6, confers gelatin photocrosslinking properties with the assistance of a water-soluble photoinitiator and exposure to light, due to the photopolymerization of the methacryloyl substituents. Some common photoinitiator are 2-hydroxy-1-[4-(2-hydroxyethoxy)phenyl]-2-methyl-1-propanone (Irgacure 2959) and lithium acylphosphinate salt (LAP). This polymerization can take place at mild conditions (room temperature, neutral pH,

aqueous environments, etc.), and allows for temporal and spatial control of the reaction [35].

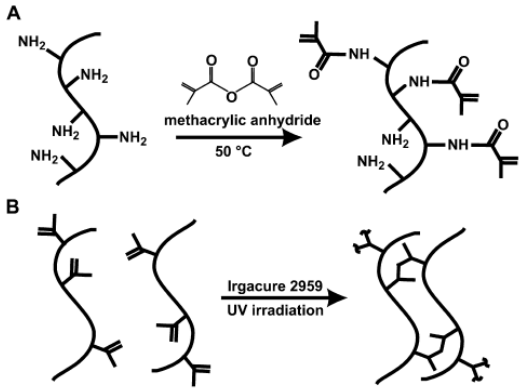

Figure 1.6: *Synthesis of methacrylated gelatin. Gelatin macromers containing primary amine groups were reacted with methacrylic anhydride (MA) to add methacrylate pendant groups [36].*

The chemical modification of gelatin by methacrylic anhydride (MA) generally only involves less than 5% of the amino acid residues in molar ratio, which implies that most of the functional amino acid motifs (such as the RGD motifs and MMP-degradable motifs) will not be significantly influenced. This means that GelMA also favors cell adhesion, proliferation, and migration [36].

1.3.4 PLURONIC®

Pluronic® (also known as poloxamer) is a triblock copolymer consisting of a central poly (propylene oxide) (PPO) block flanked by poly(ethylene oxide) (PEO) blocks; its general chemical structure is shown in Figure 1.7.

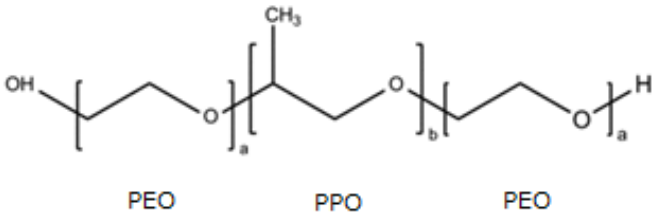

Figure 1.7: *Pluronic® block copolymers PEO-PPO-PEO*

A variety of Pluronic® is available on the market, differing for the molecular weight of the building blocks and the ratio between hydrophobic (PPO) and hydrophilic (PEO) units [37]. Pluronic® is a thermo-sensitive polymer with inverse thermo-gelling properties compared to gelatin-based hydrogels. At low temperatures (below 10°C) a solution of Pluronic® is liquid, whereas at room temperature it forms a soft, physical gel. Due to his sol-gel behavior, Pluronic® has been used as drug carrier, wound dressing, and in 3D printing applications as a sacrificial ink. The highly viscous nature of Pluronic® makes it a very easily printed hydrogel that can aid in the fabrication of complex multi-layered 3D structures with complicated shapes and internal architecture [37].

1.4 VASCULARIZED TISSUE MODEL

Living tissues have complex mass transport requirements that are principally met by blood flow through multiscale vascular networks of the cardiovascular system. Such vessels deliver nutrients and oxygen and remove metabolic by products from all the organ systems in the body. For many years, the generation of living model tissues containing even a rudimentary vascular network has constituted one of the central challenges within regenerative medicine and tissue engineering. While robust whole-organ vascularization remains a major hurdle, a broadening suite of fabrication tools has been introduced recently that can produce soft and cell-laden materials with networks of embedded perfusable channels. The purpose of creating vascularized channels running through the structure is to mimic a vascular network capable of efficiently and uniformly delivering nutrients to cells while also removing waste [39].

1.4.1 SACRIFICIAL BIOPRINTING

The current inability to fabricate thick tissues has been attributed to insufficient integration of the implanted tissue construct to the host vasculature and/or the lack of endogenous, engineered vasculature or nutrient channels in the engineered tissues. Without a vasculature system, the size of a tissue-engineered construct

is limited by the diffusional limit of oxygen required for cellular metabolism (100–200 μm) [40]. To overcome challenges associated with the lack of structural support in fabricating hollow tube constructs, which mimic the vessels, a typical approach is to print sacrificial channels (method known as sacrificial bioprinting). As reported in Figure 1.8, the vascular network is filled by a fugitive bioink that can be removed by temperature variations or appropriate solvents leaving perfusable channels behind, without harming the cells in the surrounding hydrogel matrix. Materials with reversible crosslinking mechanisms are frequently employed as the sacrificial/fugitive bioink, such as Pluronic® F127, agarose, and gelatin. The sacrificial bioprinting approaches have led to the creation of 3D vascularized tissues with robust structural, complex network and functional integrities [41],[42].

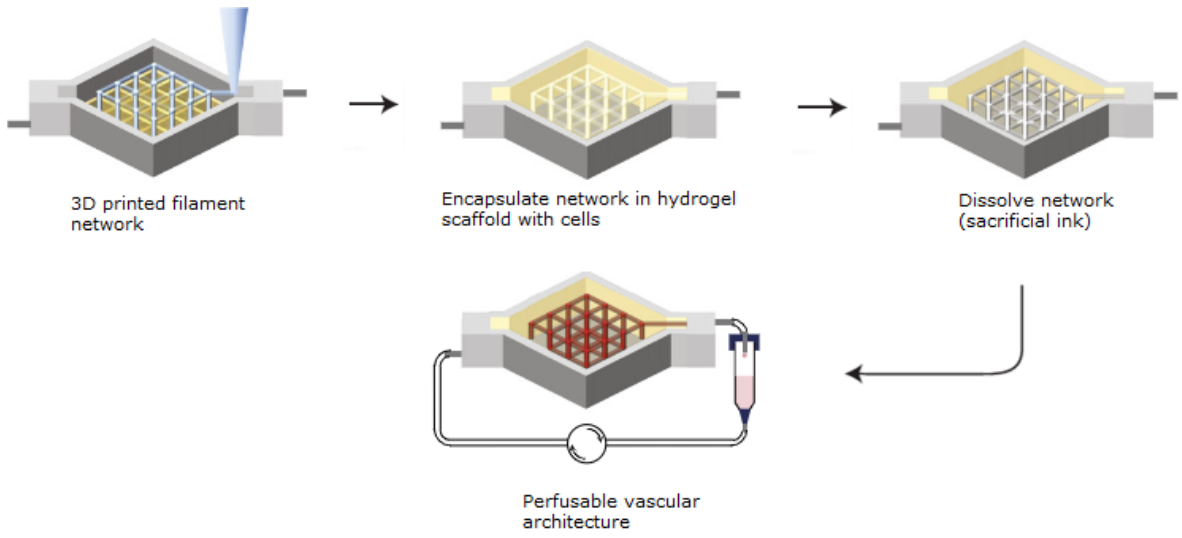

Figure 1.8: *fundamental steps to create a vascularized construct using sacrificial bioprinting method. Adapted from [43].*

1.4.2 ENDOTHELIALIZATION

Blood vessels are hollow round tubes that feed blood to various organs and tissues. The tubes branch from aorta (≈2 cm in diameter, composed by thick flexible walls able to hold the high pressure) into smaller and smaller pipelines, which ultimately form dense and small capillaries (5–10 μm in diameter). Not only varying in diameters, these vessels also possess different wall components, thicknesses, mechanical properties, permeability, and geometries, as shown in

Figure 1.9[44]. Indeed, unlike arteries and veins, capillary walls consist of a single layer of flattened endothelial cells. The vascular wall, with its complicated architecture and unique mechanical properties, is mainly composed by three types of cells: endothelial cells (ECs), smooth muscle cells (SMCs) and adventitial fibroblasts. Among them, ECs play a pivotal role in keeping the integrity of the vessel and maintaining its mechanical properties. The endothelium layer provides a continuous selectively permeable, thrombo-resistant barrier that facilitates laminar blood flow through the vessel. It also controls vessel tone, platelet activation, adhesion and aggregation, leukocyte adhesion and SMCs migration and proliferation [44],[45].

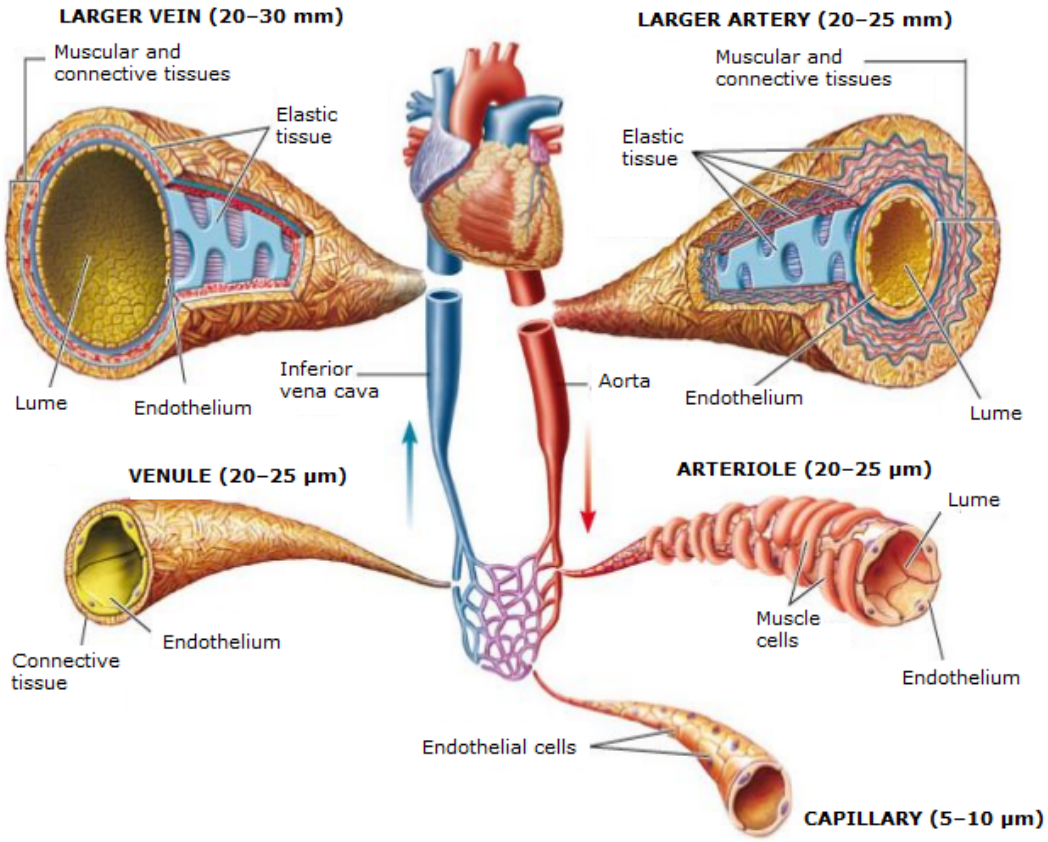

Figure 1.9*: Blood vessels composition with diameter range.*

These diverse characteristics of blood vessels are essential to serve for their specific intricate tissue/organ functions. To recapitulate these features, it is necessary to fabricate perfusable microchannels in biomimetic sizes and geometries inside the engineered tissues with proper biological components.

Primarily, two methods involving sacrificial printing are used for endothelialization of channels within scaffolds:

- post-seeding endothelialization
- *in-situ* seeding endothelialization

Post-seeding endothelialization

This type of approach requires that a network of sacrificial material is initially printed within the hydrogel scaffold. The fugitive ink, which defines the embedded vascular network, is often Pluronic® F-127 40% w/v in PBS. As mentioned in section 1.3.4, taking advantage of the material's characteristic physical properties, this ink can be removed from the fabricated tissue upon cooling to 4 °C, where it undergoes a gel-sol transition. The entire structure, once stabilized by crosslinking methods, can be refrigerated or immersed in a cold liquid (usually PBS or water) to remove Pluronic®. This process yields a perfusable network of inter-connected channels, which can be then coated with endothelial cells. The key aspect is that no cells are used in the printing step to create the channel, but are seeded once the sacrificial material has been removed. This requires high numbers of cells for the endothelialization, reaching densities up and above $3 \cdot 10^7$ cells/mL_{medium}.
While this method has yielded impressive results, the use of a typical four step-process (printing, casting, template removal, post-seeding) loses many of the key advantages of single-step 3D bioprinting, such as the speed and the simplicity. Also, post-seeding is a poorly controlled step that sometimes results in a nonuniform distribution of cells throughout the templated channels [44],[46].

In-situ seeding endothelialization

The *in-situ* endothelialization method can produce endothelium with a far greater cell seeding uniformity than can be achieved using the conventional post-seeding approach seen before.
The *in-situ* strategy, sketched in Figure 1.10, enables the fabrication of 3D complex vascular networks using a single bioprinting step, without the need of cell post-seeding. The endothelial cells are already embedded inside the sacrificial bioink used in the initial printing step. The sacrificial bioink and a crosslinkable

matrix bioink are printed side by side into 3D structures. After crosslinking the construct, the printed structure can be incubated and turned over at regular intervals for several hours to allow the fugitive ink to liquefy and the cells in it to adhere to the created channel wall.

The most used endothelial cells in literature are HUVECs (Human Umbilical Vein Endothelial Cells), here seeded with a density of $5 \cdot 10^6$ cells/mL_{gel}, lower than that required for post-seeding protocols [46].

On the other hand, because of the shear stress generated during the printing phase, cell viability might be affected, thus representing the greatest disadvantage of this endothelialization method.

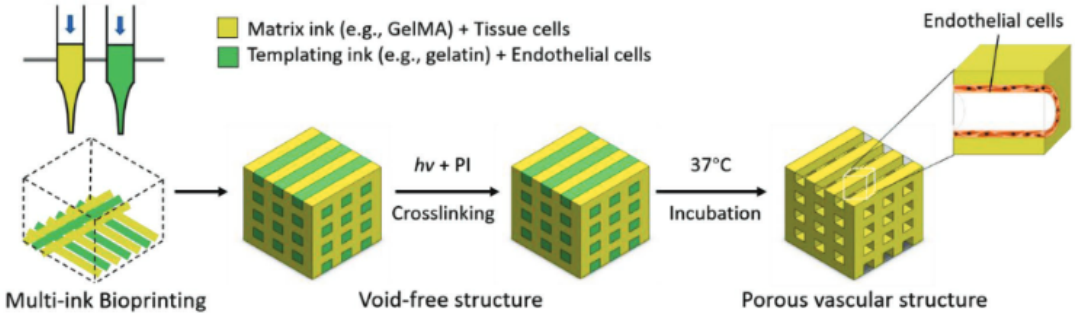

Figure 1.10*: schematization of the process of In-situ seeding endothelialization [46].*

1.5 AIM OF THE THESIS

The purpose of this thesis is the creation of a vascularized and endothelialized construct fabricated via 3D bioprinting. The goal is to develop the ideal protocol for creating perfusable channels using bioprinting alone, without the need of casting. Therefore, it will be important to evaluate the correct printing parameters and the right characteristics of the hydrogels to be used.

In this thesis, the sacrificial bioprinting method will be analyzed. Therefore, two materials will be used: GelMA as matrix, and Pluronic® F-127 as sacrificial bioink. In addition to the printing parameters, particular geometries will also be evaluated to make the endothelialization protocol easier and more replicable.

The work will be biologically validated using cell lines such as HUVECs and MSCs, present only in the channel or both in the channel and in the GelMA matrix. In this way, it will be possible to evaluate the proper perfusion of the medium through the channel, the transport of nutrients throughout the whole construct, and the behavior of the cells when subjected to continuous flow. This approach allows to perform studies that are clearly more realistic because they refer to three-dimensional models.

Chapter 2
MATERIALS AND METHODS

This chapter will introduce the main methods and protocols concerning the basic steps in the development of this thesis.
Initially, the synthesis and preparation of the main material, gelatin methacrylate GelMA, will be described. Then, the concept of the structure will be introduced, starting from the CAD design to the actual printing of the channeled construct . The last section will be devoted to the protocols inherent to the cell lines used; in detail, protocols for studying cell behavior after several days of perfusion will be illustrated.

2.1 HYDROGELS

As mentioned earlier, the main materials that will be used in this thesis during the printing process are hydrogels. Due to their high biocompatibility and biodegradability, gelatin methacrylate and Pluronic® F-127 were chosen. It is important to report how the preparation of these materials takes place as even small variations in the synthesis process can affect their properties and those of the desired final product.

2.1.1 GelMA SYNTHESIS

The gelatin used in this thesis is a type A gelatin derived from porcine skin. This type of gelatin is obtained from collagen that is hydrolyzed into protein fragments by acid treatment (Sigma Aldrich®, G1890).
Literature articles show different protocols to produce GelMA; the one used in this thesis refers to specific insights included in the study by Shirahama *et al*. [47].
GelMA is obtained through a reaction between type A gelatin and methacrylic anhydride (MAA), also provided by Sigma Aldrich®. This reaction introduces methacrylic substitution groups on the reactive amine and hydroxyl groups of the amino acid residues, as shown in Figure 2.1 below.

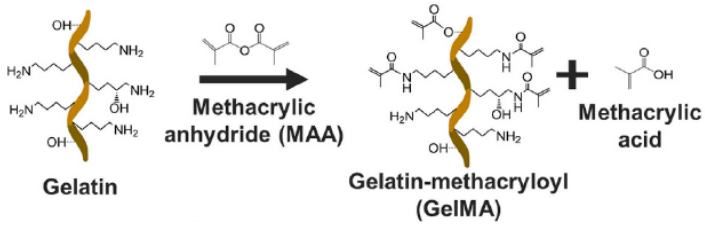

Figure 2.1: *GelMA synthesis [47].*

Several are the conditions to be controlled during the synthesis process, which include temperature, pH, MAA concentration, gelatin concentration, and time.
After dissolving gelatin in a 0.25 M sodium carbonate-bicarbonate buffer (CB buffer) at 40°C under stirring at 800 rpm, MAA was added dropwise to the solution in an amount ranging from 15 to 50 µL per gram of gelatin. The amount of MAA used affects the degree of functionalization, also called the degree of substitution (DS), that is to be achieved (from 25% to 75%, respectively). The degree of substitution is defined as the amount of methacrylic anhydride molecules that can react with the lysine groups of the gelatin itself. Following previous studies conducted in the laboratory, a degree of functionalization of 70% was chosen for this thesis. As shown in Figure 2.2 the study performed showed that a DS plateau state is reached after 1 hour from the start of the reaction. Despite this, a duration of 2 hours was chosen for our synthesis, maintaining a constant temperature of 40°C and constant agitation of 800 rpm. This longer time allows us to have total certainty that the reaction occurred in the correct manner, avoiding inhomogeneity in volume.

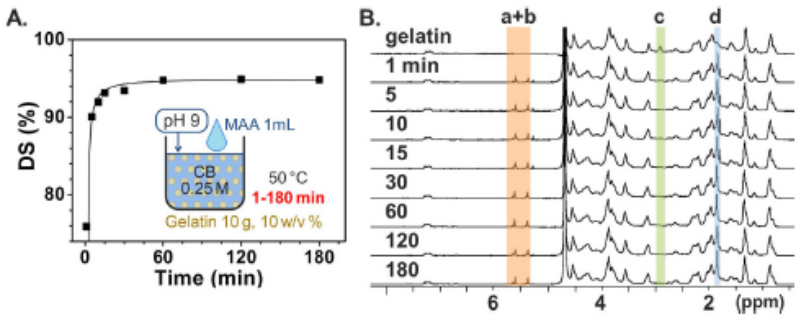

Figure 2.2: *A) DS versus reaction time. B) HNMR verification [47].*

After 2 hours, hydrochloric acid (also from Sigma Aldrich®) is added to stop the substitution process and set the pH to a physiological value of 7.4. Then, it is

required to perform a purification step of the solution from the waste products (methacrylic acid) and excess reagents. To do this, the obtained GelMA is dialyzed for 4 days inside special dialysis membranes with 14 kDa molecular weight cut-off (MWCO). Dialysis is carried out keeping the membranes at constant temperature of 40°C and agitation of 200 rpm in ultrapure Milli-Q water (purified and deionized by a system made by the Millipore Corporation®). Water needs to be changed at least three times a day to ensure the efficiency of the process.
The last step of synthesis involves freeze-drying the GelMA for 7 days to obtain a solid material that will be possible to use at the desired concentrations, for up to six months. Freeze-drying is a process that allows the removal of water from a solution with the least possible deterioration of the structure and components of the substance itself. It is therefore essential, once the final product has been obtained, to keep it sheltered from humid conditions. These could cause a rehydration of GelMA and thus a change in the properties of the material.
The full protocol of the synthesis is listed in detail here:

- 0.25 M CB buffer preparation:
  - in 200 mL of Milli-Q water dissolve 1.6 g of Sodium Carbonate (Na_2CO_3) and 3 g of Sodium Bicarbonate ($NaHCO_3$);
- weigh the gelatin: a 10% w/v solution of gelatin in CB buffer is request;
- dissolve gelatin in CB buffer at 40°C and 800 rpm for about 20 min;
- the pH should be around 9.2-9.4: check it. If it’s higher, lower it by adding hydrochloric acid HCl;
- add methacrylic anhydride drop by drop in varying amounts according to the DS you want to achieve;
- let the reaction take place for two hours at 40°C and 800 rpm;
- after the two hours pH should be around 8.3: check it;
- add HCl all at once near the fluid surface to block the reaction and set the pH to a physiological value of approximately 7.4;
- dilute the product in milli-Q water: this step will allow the solution to be more easily filtered in the final step;
- sterilize dialysis membranes by immersing them in boiling milli-Q water for 5 minutes;
- pour GelMA into the membranes and seal them. Immerse the membranes in enough milli-Q water to cover them completely. Leave the membranes

in water at 40°C and about 200 rpm for 4 days, changing the water at least three times a day. At each water change, turn the membranes upside down to prevent deposits formation;

- filter GelMA and transfer it to a Falcon® with a 0.22 µm filter cap. Then freeze-dry it for 7 days. After that use Parafilm® to cover the filter cap and prevent the passage of moisture.

2.1.2 HYDROGELS PREPARATION

This section will briefly discuss how materials are prepared and stored for later use in the bioprinting process. The various steps that enable the transition from raw material to ready-to-use product will then be listed.

GelMA preparation

Once GelMA is detached from the freeze-dryer, the product appears as a white solid with a polystyrene-like consistency, as in Figure 2.3. GelMA, obtained according to the synthesis process described above, can be stored in a freezer at a temperature of -20°C and protected from humidity. This keeps the properties of the material stable for up to six months and allows it to be used at different concentrations as needed.

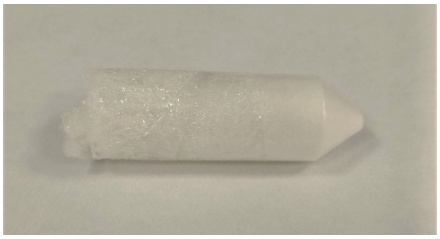

Figure 2.3*: resulting GelMA lyophilized*

To use GelMA as a gel for bioprinting purposes, it must be dissolved in a solvent. In this thesis, we used is 1xPBS and the concentration of the final GelMA solution is 8% w/v.

In addition, for the UV-crosslinking process to occur, a photoinitiator must be introduced: we used Irgacure 2959 (from Sigma Aldrich®) in a concentration of

0.5%, following previous studies conducted in the laboratory. A change in the photoinitiator was also evaluated: LAP (lithium acylphosphinate salt) at a concentration of 0.1% was used for some preliminary printing tests.
The GelMA preparation protocol is listed here:

- weigh the desired amount of GelMA in total sterility;
- calculate the volume of 1xPBS to obtain a 8% w/v GelMA concentration;
- calculate the amount of Irgacure 2959 to obtain a concentration of 0.5% w/v. If using LAP, calculate the amount to get a concentration of 0.1% w/v;
- dissolve the photoinitiator in 1xPBS at a constant temperature of 40°C and agitation of 400 rpm for about 20 min. Avoid evaporation using Parafilm® to seal the Becker in which the mixing takes place;
- filter the photoinitiator-1xPBS solution into the Falcon® in which the GelMA is contained to maintain sterility;
- use a vortex mixer to favor complete dissolution of GelMA in the mixture;
- centrifuge the hydrogel for 5 min at 3500 rpm to eliminate gas bubbles.

Appendix A.1 shows the most relevant results of some mechanical tests carried out on GelMA in previous studies performed in the laboratory.

Pluronic® F-127 preparation

Preparing Pluronic® is a quick and simple process. As mentioned in Section 1.3.4, Pluronic® F-127 is a thermoreversible material: this means that at temperatures below 10°C it appears as a liquid, and is solid at higher temperatures. As said before, by exploiting this ability of Pluronic® F-127, we created a channel through the sacrificial bioprinting approach. At first, it is necessary to evaluate the printability of the material itself, determining the ideal concentration to dissolve in the solvent (usually 1xPBS). Through previous studies in the laboratory, it was possible to conclude that the optimal concentration of dissolved Pluronic® F-127 is 30-40% w/v. For this thesis, a concentration of 40% w/v was chosen.
The preparation protocol is summarized here:

- choose the amount of 1xPBS in which to dissolve the Pluronic® F-127;
- weigh the amount of Pluronic® F-127 powder to ensure a concentration of 40% w/v;

- dissolve Pluronic® F-127 in 1xPBS leaving it at 4°C in the refrigerator and stirring it;
- use a liquid autoclave to sterilize the resulting hydrogel: this step is extremely difficult due to the rapid gelling of the material;
- store the material in a refrigerator at a temperature of 4°C until use.

2.2 3D BIOPRINTING

This section will discuss the methods and design steps that allowed us to achieve results in the generation of the vascular channel. We will also describe the development of a special clamp that allows the construct to be printed inside and kept stable and isolated, thus sterile, for the entire duration of the experiment. The ideal printing conditions of the materials used will then be discussed, with the aim of setting the correct parameters and making the bioprinting replicable.

Before doing so, it is necessary to make a small detour concerning the available equipment. The laboratory is equipped with a 3D printer, the BioX from the company Cellink®. It is an extrusion printer characterized by extreme versatility: the three printheads can be used in combined and simultaneous action; in this way, more complex and efficient multi-material three-dimensional bioprinting can be performed. BioX's three printheads are interchangeable and specially designed to guarantee a printing resolution of 1 μm under perfectly controlled conditions. In the case of temperature-sensitive materials, it is possible to use a temperature-controlled head that modulates the temperature in a range of 4-250°C. It is also possible to set the print bed temperature from 4°C to 60°C. The printer is also equipped with photo curing tool heads at three different wavelengths; this allows you to use UV modules at 365 nm, 405 nm, and 465 nm, depending on the hydrogel you want to crosslink.

The printing action is provided by an internal compressor that pushes air to the printheads, allowing it to reach 200 kPa. Since the internal tubes can sustain a maximum pressure of 700 kPa and, as we will see later, the materials we will use require a higher pressure than the one provided by the BioX, an external compressor was chosen to supply the bioprinter.

Final important feature, the BioX is equipped with dual high-power fans that create a powerful airflow through its dual-filtration top, creating a positive air pressure

inside the chamber and creating a complete system that maintains sterility inside the machine.
All the main characteristics listed are summarized in Figure 2.4 below.

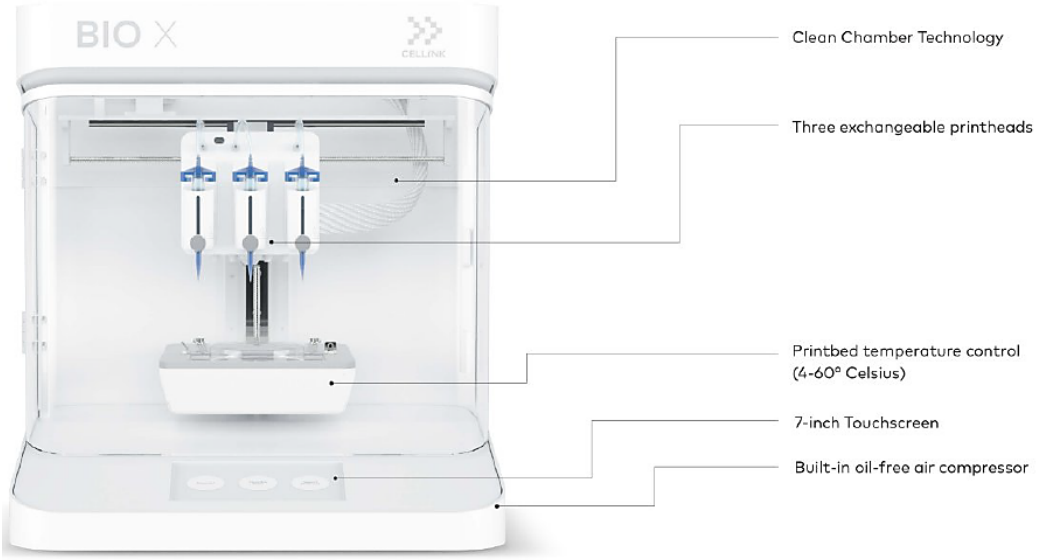

Figure 2.4*: BioX 3D bioprinter from Cellink® company.*

2.2.1 STRUCTURE DESIGN

The design of the structure chosen for this thesis was done using computer-aided design software, AutoCAD. The design was then exported to an STL file (STereo Lithography interface format or acronym of "Standard Triangulation Language") and imported into another program capable of converting the file to a G-Code. G-Code is nothing more than a programming language, such as Python, MATLAB, C++ and others, that is used in the definition of a numerically controlled machine path and that enables 3D printing, as it provides all the necessary information (in terms of position and movements) to be followed by the printer during the process. Among the different types of software that enable this type of conversion (STL to G-Code), we used *PrusaSlicer* thanks to his easy to-use interface. It allows to easily set many printing parameters, like the possibility to specify the size of the nozzle, the height of each layer and the infill pattern (geometry and percentage).

CAD model of construct

Following previous studies carried out in the laboratory on different types of structures, the design of the construct whose purpose is to contain a channel in which cellular medium can flow, is focused on a serpentine embedded in a parallelepiped as shown in Figure 2.5 below. Some changes have been made to the original model; the choice of extending the end of the serpentine outside the structure will be explained later.

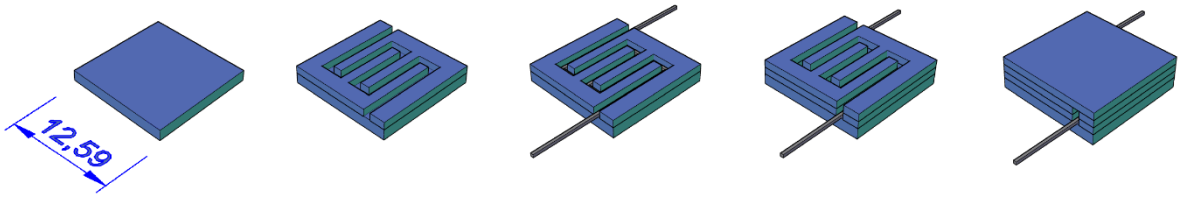

Figure 2.5*: serpentine inside a 12.59x12.59x3.6 mm parallelepiped.*

Thanks to the figure above, it is also possible to understand the main steps implemented during the printing process. Initially, the layer for the base of the parallelepiped is printed, using GelMA; this is followed by an additional layer that serves as the container of the Pluronic®. Next, the printhead changes switching to Pluronic® and print the serpentine. The last two steps involve another layer as Pluronic® container and the final covering with GelMA.
Considering a standard internal extruder with diameter of 0.25 mm (25G) for GelMA bioprinting, the size of the structure is 12.59x12.59x3.6 mm, not taking the extending end of serpentine into account. For Pluronic® we chose an internal extruder diameter of 0.25 mm (25G) or 0.21 mm (27G) for a greater printing precision.

G-Code generation of construct

As mentioned earlier, once the CAD model has been made, it is necessary to export it to an STL file. In this way, with the use of special software such as *PrusaSlicer*, all the main print settings can be chosen to export the correct G-Code

file. As said, the G-code file contains the instructions that the bioprinter should execute to create the structure.
Figure 2.6 shows the view that appears using *PrusaSlicer* program: blue indicates the structure printed using the first printhead, the GelMA one, while red shows the serpentine printed using the second printhead, the Pluronic® one.

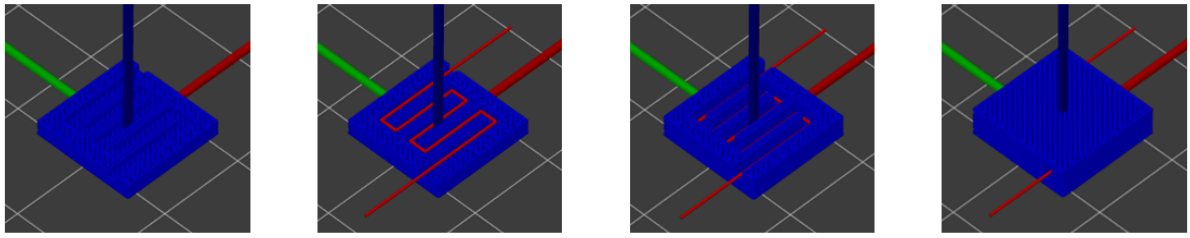

Figure 2.6*: printing sequence of serpentine inside parallelepiped in PrusaSlicer window. In blue there is GelMA structure, in red Pluronic® F-127 serpentine.*

The most significant parameters that can be changed in the program are listed here:

- Filament diameter: 0.25 mm;
- Layer height: 0.4 mm;
- Fill density: 80%;
- Fill pattern: Rectilinear;
- PH1 speed: 5 mm/s;
- PH2 speed: 4 mm/s.

It is interesting to note that the software does not allow the filament diameter to vary between the two printheads. This means that there is a discrepancy in case a 27G (0.21 mm) tip was used to print the Pluronic®; however, this detail is not going to affect the success of the print itself.

CLAMP model

As mentioned in Section 1.4.1, to create the vascular channel lined with endothelial tissue and subsequently perfused, the sacrificial bioprinting method was chosen. Taking advantage of the thermoreversibility properties of Pluronic®,

which are opposite to those of GelMA, once the structure is printed it is necessary to remove the Pluronic® serpentine from the construct. This creates an empty channel that will later be filled with cells.

Perfusion requires the insertion of needles (connected to tubings leading to the medium reservoir and the peristaltic pump) in the channels. One of the major challenges was to properly insert the needles inside the channel and keep them stable, preventing them from shifting or slipping out during the wash-out of Pluronic®, seeding of cells, and perfusion of the entire construct. The stability of the needles is extremely important: even small shifts can cause the experiment to fail as the nutrients are no longer correctly distributed within the channel, and attempting to touch the needles to reposition them, would mean risking contaminations. In addition, leakage would significantly increase the amount of media used/wasted.

For this purpose, a special clamp was designed, again using AutoCAD. The construct made of GelMA and Pluronic® is printed directly inside of it, then covered with a thin layer of PDMS (polydimethylsiloxane obtained by designing the negative of the printed construct) and finally closed with screws by the top layer of the clamp. PDMS, which is biocompatible and gas permeable, allows to isolate the printed structure and avoid possible contamination, while keeping a proper supply of O_2 and CO_2 to the structure. Holes with a diameter corresponding to the needles used were created at the sides of the clamp to house them: by inserting the needles after printing and closing, they directly and precisely reach the beginning and end the of the printed serpentine. For greater safety, it was decided to elongate the two ends of the serpentine: in this way Pluronic® will be printed initially on the clamp itself, more precisely on the guides in which the needles will then be placed, making their insertion easier.

The main components of the clamp can be seen in Figure 2.7 below.

Once the CAD model is finalized, it is necessary to export the STL file and then obtain the final G-Code thanks to the *PrusaSlicer* software. The clamp was printed in a particular material called ULTEM™ 1010 from Stratasys®. This is a high-performance thermoplastic polyetherimide (PEI) 3D printer resin that has high heat resistance while having the lowest thermal expansion coefficient among FDM (fused deposition modelling) materials. In addition to having high strength properties, ULTEM™ 1010 resin is a perfect material for complex applications, is biocompatible and autoclavable (thus sterilizable).

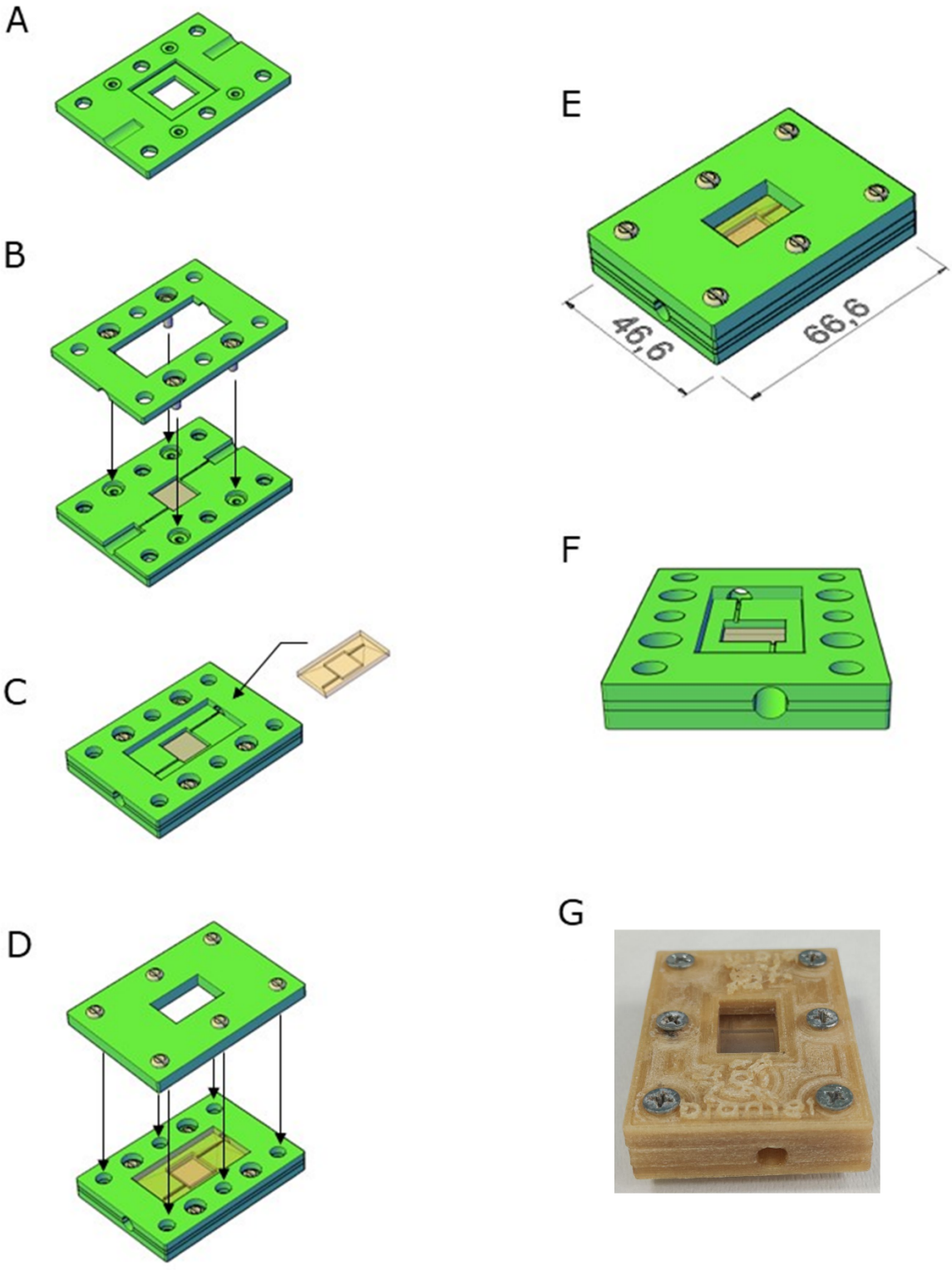

Figure 2.7*: main components of the clamp. A) base of the clamp; B) addition of glass slides and second layer of the clamp with nozzles guide; third layer of the clamp stopped with screws; C) after printing, addition of PDMS cover; D) top layer of the clamp stopped; E) clamp measurements; F) clamp side inlet; G) clamp printed using ULTEM™ 1010.*

2.2.2 GelMA AND PLURONIC® GENERAL PRINT PROPERTIES

Considering that the materials used in this thesis, GelMA and Pluronic®, have different behaviors, it is necessary to investigate their characteristics regarding the printing process.

GelMA is a thermo-reversible material that is liquid above 25-30°C and gels at lower temperatures. This is due to the physical bonds that are formed between the polymer chains (sol-gel transition); reversible bonds that can be broken by increasing temperatures and returning the material to a solution condition (gel-sol transition).

For temperatures below 20°C, GelMA takes on the characteristics of a high-viscosity gel, requiring large increases in the printing pressure and resulting in a loss of print definition. When the temperature exceeds 25°C GelMA tends more towards a liquid and is practically impossible to print and hold a shape. The challenge during the printing process is therefore to find and maintain the correct temperature so that the right pressure and consistency of the material are balanced. We generally choose to print at a temperature of 23.5$\pm$1°C, to work with a gelatinous material with correct viscosity that can be printed accurately without requiring high pressures. Printing pressure is a key parameter in the case of GelMA: when the material also contains cells, high pressure can lead to lethal shear stresses to the cells, causing their death.

A temperature-controlled printhead is used to ensure maintenance of the correct temperature during the printing process: equipped with an internal fan, it can cool or heat the syringe loaded with the material. Since positioning of the syringes in the temperature-controlled print heads is not rapid, it is recommended to refrigerate GelMA at 4°C for about 5 minutes to accelerate the gelation process before placing the cartridge in the printhead. To ensure good stability of the printed structure, the temperature of the printing bed can also be set to about 22°C. In this way, the lower layers begin physical cross-linking in advance, which allows for better success and solidity of the print.

Once the desired construct has been obtained, chemical crosslinking can be performed; using UV light, permanent and irreversible intermolecular junctions are formed. Depending on the choice of photoinitiator used and the distance between the print and the UV source, the time required for complete crosslinking

varies. In general, an exposure of approximately 60 seconds is sufficient to ensure complete crosslinking of the structure.
Pluronic® is also a thermo-reversible material, but it has opposite characteristics to those just seen for GelMA and its printability is less temperature dependent. At temperatures below 10°C the material appears as a liquid, thus impossible to print, while at temperatures above 15°C it is a gel. It follows that at room temperature Pluronic® can be easily printed, with excellent resolution and with pressures dependent on the needles used. As mentioned earlier, is possible to set the temperature of the printing bed: it is important not to go below 15°C to avoid that the Pluronic® starts to liquefy during the printing phase.
Briefly summarized, the process consists in printing GelMA at approximately 23.5°C, followed by Pluronic® at room temperature; then the entire print is exposed to UV light. Taking advantage of the opposing characteristics of thermo-reversibility, the construct is briefly placed at temperature lower than 10°C to allow Pluronic® to dissolve and, after a wash-out, to remove the excess.

2.2.3 3D BIOPRINTING OF VASCULAR CHANNEL

The main steps to produce a cell-laden vascularized structure can be seen in Figure 2.8, Figure 2.10 and are summarized as:

1. GelMA and Pluronic® preparation;
2. calibration and setting of the bioprinter;
3. multi-material bioprinting and GelMA crosslinking;
4. Pluronic® liquefaction and washout.

The first item on the list has already been extensively covered in Section 2.2.2 so, below, the remaining three passes will be explained.
.

Calibration and setting of the bioprinter

After loading the materials into the appropriate printing syringe, the printer needs to be set up. First, the G-Code file must be loaded in the printer via external USB flash drive. This will allow to select the desired printing protocol and access the

printing window choosing the initial configuration regarding the type of printheads, and the temperatures for the printheads and the print bed. The critical stage of the setup process is calibration, a delicate and at times complicated step, crucial to achieving printing success. Given that our protocol involves the use of two materials therefore of two separate printheads, the challenge is to exactly calibrate the two syringes at the same point, with coordinates (0,0,0); in case the calibration is offset, the result will not be the desired one. Calibration is performed moving the extruders along the three main axes *x, y, z*, leaving a height between the needle and the bed comparable to that of a sheet of paper (about 200 μm).
The last step before the actual printing is te choice of the extrusion speed and pressure. Generally, a standard speed of 5 mm/s is chosen for GelMA while 4 mm/s is chosen for Pluronic®, regardless of the type of needle used. The pressure, on the other hand, is highly dependent on the diameter of the needle and the viscosity of the material, so it must be verified each time experiments are done. For GelMA at 24°C, it is expected to print at a pressure of 20-50 kPa, while Pluronic® is printed at a much higher pressure of about 400-600 kPa, with a 25G and a 27G respectively.

Multi-material bioprinting and GelMA crosslinking

After calibrating the printer and setting the temperature, speed, and printing pressure, the bioprinting begins. As shown in Figure 2.6, the printing will proceed layer by layer, alternating the two different printing heads, until the structure is completed. Once the printing is complete, the final step id the exposure of the entire construct to UV light as seen in Figure 2.8. For this purpose, it is necessary to operate with the general lights off and activate the correct wavelength: Irgacure requires a wavelength of 365 nm; while LAP needs 405 nm. Moving along the main directions of the print bed, it is essential to place the light output in the center of the print so that it is fully irradiated. To ensure that the structure is completely crosslinked and to reduce time, it is advisable to raise the print bed as high as possible. In case the GelMA is loaded with cells, reducing the exposure time to UV light is essential to avoid cell death, as these particular wavelengths, if prolonged, are not cell friendly.

Considering the shorter distance between the structure and the light output and the height of our structure, when using Irgacure 60 seconds of UV are enough to complete the crosslink; in the case of LAP 30 seconds are sufficient.

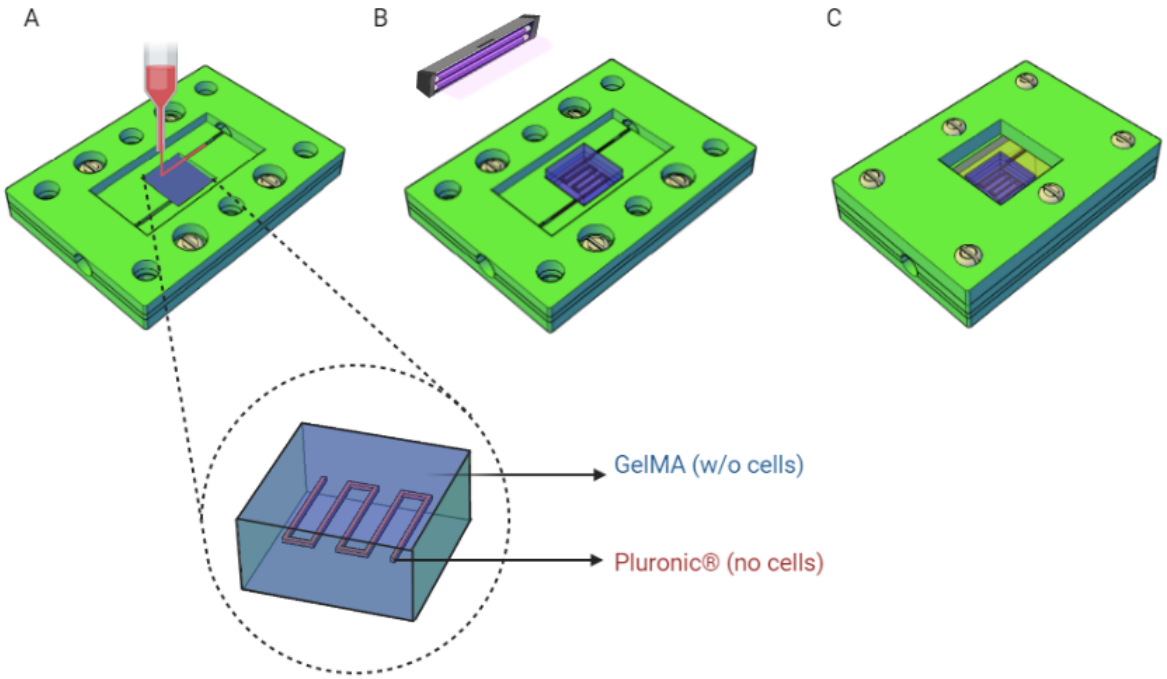

Figure 2.8*: GelMA and Pluronic® printing (A) and subsequent UV crosslinking (B). Complete closure of the clamp (C.).*

Pluronic® liquefaction and washout

After cross-linking, covering with PDMS and closing the clamp, it is necessary to remove the Pluronic® from the channel. Taking advantage of the material's thermoreversibility, by placing the clamp in the refrigerator at a temperature of 4°C for about 5 minutes the Pluronic® begins to liquefy. To completely remove all traces of Pluronic®, it is essential to wash it out injecting cold 1xPBS in the serpentine using the clamp inlets to insert the needles, which will insert exactly where Pluronic® was printed, as schematized in Figure 2.9. Considering that the serpentine is printed using a 25G nozzle, wash-out was done using 22G flexible-tipped needles.

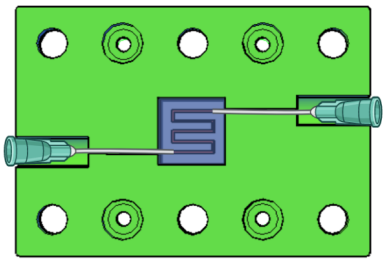

Figure 2.9*: perfect match between needles and Pluronic® serpentine.*

One needle is used as the inlet from which the 1xPBS will be injected very slowly, via a syringe, while the other will be used as the outlet from which the injected liquid containing the residual Pluronic® will flow out. The procedure is shown in Figure 2.10.

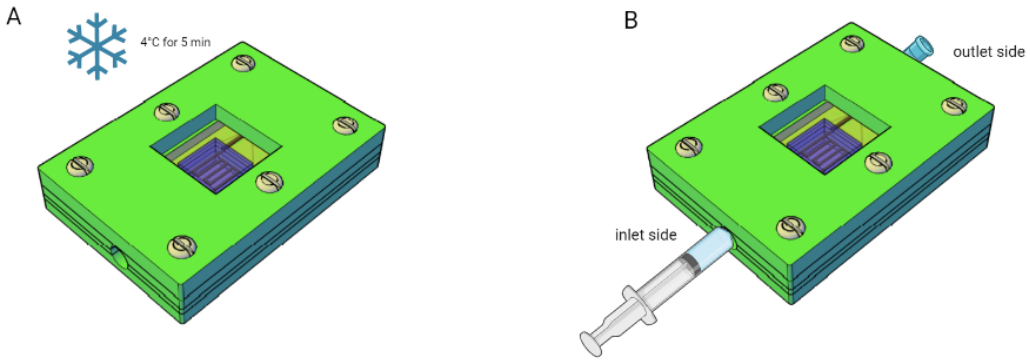

Figure 2.10*: Pluronic® liquefaction at 4°C for 5 minutes (A) and wash-out with 1xPBS (B).*

2.3 BIOLOGICAL VALIDATION

As mentioned above, the purpose of this thesis is to create a perfusable vascularized channel embedded in a 3D cellularized structure to delivery nutrients to the cells that are present in the matrix. In addition, to mimic the behavior of a capillary system, the channel surface can be lined with endothelial cells to recreate the endothelial barrier that separates the flow of medium from the cells. In section 2.2.3, we have seen how multi-material bioprinting is performed; here we will go into the biological significance of the study, examining the cell culture, seeding and analysis protocols of the experiment.

2.3.1 CELL LINES FOR ENDOTHELIALIZATION

The cell types used in this thesis are human umbilical vein endothelial cell (HUVEC) and human mesenchymal stem cell (MSC).

HUVECs are cells derived from human umbilical cord, widely used as a model for the study of vascular endothelium properties and the main biological pathways involved in endothelium function. MSCs are isolated from the bone marrow (recently also from adipose tissue, placenta, and umbilical cord) and useful in research and clinical therapy because they can modulate the immune system during wound healing, repair tissue, and exert anti-fibrotic activity. Both cell types are characterized by some extent of self-renewal and potency; self-renewal defines the ability of a cell to generate an undifferentiated exact copy of itself. While potency identifies the ability of a cell to differentiate into other specialized cell types. The main difference between the two lines is that MSCs are primitive, undifferentiated cells that exhibit multilineage differentiation capacities that, under specific conditions, can give rise to bone, cartilage, adipose tissue, neuron, muscle, and endothelial cells; in contrast, HUVECs only have the ability to differentiate into endothelial cells [48],[49].

Generally, cells are cultured in a 2D environment, such as T-Flask that can have different sizes depending on the experiments to be conducted; there can be T-25, T-75 and T-150 (numbers indicate surface area in cm^2). When placed in culture Flasks, the cells appear as in Figure 2.11: HUVECs have an elongated shape while MSCs have a triangular and/or rhomboidal shape.

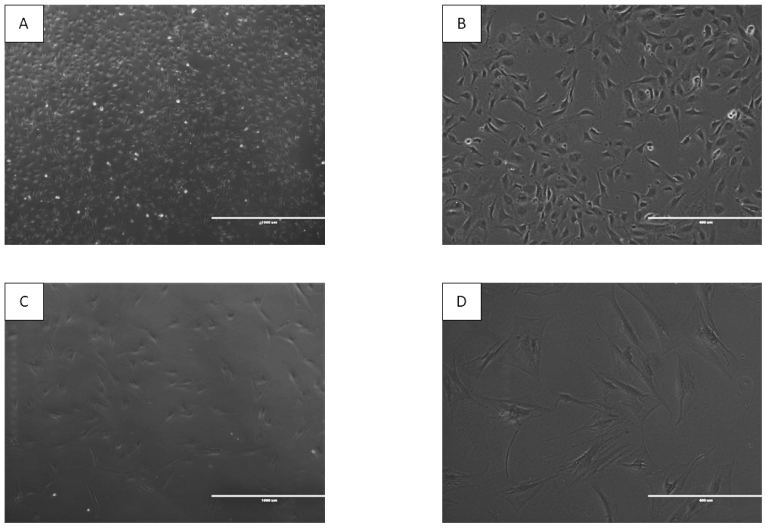

Figure 2.11*: microscope images. A) HUVECs with 4X objective; B) HUVECs at 10X; C) MSCs at 4X and D) MSCs at 10X;*

Another important difference between the two lines is the culture medium used, which is the liquid solution required for proper maintenance and proliferation of the cells. HUVECs require the Endothelial Cell Growth Medium 2 from PromoCell® that is a low-serum (2% v/v) medium that contains Insulin-like Growth Factor (Long R3 IGF), Vascular Endothelial Growth Factor (VEGF), specific supplement and Penicillin-streptomycin Mixture. MesenCult™ Basal Medium from StemCells Technologies® is standardized for the culture of mesenchymal stem cells; this kit includes the basal medium, the specific supplement and L-Glutamine.
All culture media also contain a pH indicator, usually phenol red: at physiological pH the solution is pink, while at acid pH it veers towards yellow. Presence of bacterial contamination within the culture or accumulation of excessive waste products generated by dying cells cause changes in pH, from physiological to acid, leading to a change in color. Color shifts, even in the absence of contamination, indicates that the culture medium needs to be replaced.

2.3.2 DETACHMENT AND CELL ENCAPSULATION IN GelMA

When cells reach the desired confluence, *i.e.* they have proliferated to the point that they have covered most of the surface of the Flask, it is necessary to detach them from the surface, count and resuspend them in new medium. These steps are extremely delicate and must be performed in total sterility inside a biological hood to avoid contamination.
To assess the percentage of confluence and estimate the density of adherent cells, it is sufficient to look at the culture Flask under a microscope and do a qualitative analysis of the image. Depending on the cell line chosen, the expected confluence percentage varies: Table 2.1 shows an approximation of the expected confluence in a T-150 for the cell lines used in this thesis.

Table 2.1*: approximation of the expected cells confluence in a T-150*

Cell line	Confluence cell number
HUVEC	$6\text{-}8 \cdot 10^6$
MSC	$2\text{-}4 \cdot 10^6$

When the confluence reaches about 80-90%, the first step is to detach the cells from the culture Flask. The medium in the Flask is completely aspirated and a wash is done for 5 minutes using 1xPBS to remove dead cells, cell debris, and calcium and magnesium ions. After the 1xPBS is aspirated, trypsin is added and the Flask is placed in a 37°C incubator for 5 minutes; if a T-150 is used, 6 mL of trypsin are added, while in case of a T-75, 3 mL are sufficient. It is important to be careful not to exceed the indicated amount, as too much of this solution could cause cell damage and death. Trypsin is an enzyme capable of cutting cell-surface protein junctions and is therefore used to detach cells, which then float in the liquid and can be retrieved by simple aspiration. Since prolonged exposure to trypsin can be harmful, after the 5 minutes incubation it is necessary to dilute it with culture medium: 14 mL of medium are added to a T-150 so that a total amount of 20 mL is reached. The amounts of trypsin and medium must be halved in a T-75, reaching a total volume of 10 mL. These solution of trypsin and medium are then taken from the flask and placed inside a Falcon® centrifuge tube. At this point it is necessary to count the cells: to do this, a 10 µL aliquot is taken from the Falcon® and mixed with 10 µL of trypan blue. Trypan is a dye that selectively stains dead cells by penetrating the cytoplasm due to the ruptured cell membrane; thus under the microscope only live cells will be bright. 10 µL of the mixture are injected into a Bürker chamber to perform a count under the microscope. The Bürker chamber is a device consisting of a grid of 9 squares; by counting the number of cells present in 3 of them and averaging ($\overline{N}$), is possible to estimate the number of cells N_C present in the original volume V placed in the Flacon®. Given 2 as the dilution factor from trypan blue, and 10^4 as the Bürker chamber correction factor, the formula for deriving N_C is:

$$N_C = \overline{N} \cdot 2 \cdot V \cdot 10^4 \tag{2.1}$$

Meanwhile, the starting solution in the Falcon® is centrifuged (1000 rpm for 5 min with soft deceleration) so that a pellet, which settles to the bottom, is separated from the liquid: the supernatant is gently removed with a pipette, paying attention not to break the pellet. Knowing the number of cells, it is possible to make the correct proportions to resuspend them in the right amount of medium. When cells are encapsulated in GelMA, to not vary the viscosity and density of the material

(and thus the printability properties), the correct ratio of resuspension of cells in a volume of medium is 1:25 with the hydrogel [50].

2.3.3 ENDOTHELIALIZATION AND PERFUSION

The goal of the thesis is to fabricate a perfusable vascularized 3D cellularized model; based on that it is useful to understand the endothelialization protocol and how perfusion of the medium through the channel is implemented.

Endothelialization protocol

As we saw in section 1.4.2, two methods are generally used to create an endothelial network inside a printed construct. Briefly, the *in situ* seeding technique involves printing the channel with cells already in the material, and the post-seeding technique used in this thesis foresees the later stage seeding of endothelial cells after the removal of the sacrificial ink. Taking advantage of the known thermoreversibility characteristics of Pluronic®, once the material has been washed-out, cells are gently injected and occupy the void left by the removal of the Pluronic®. It proves impossible to perform the experiments Using the *in situ* seeding technique would cause extensive cell death because of the high pressures needed to print the Pluronic® 40%.
After printing, cross-linking the construct, and performing the wash-out with 1xPBS, the cells, counted and resuspended in the correct amount of medium, can be gently injected into the channel.
Several endothelialization tests were performed to optimize the protocol used: variations were made in terms of the cell density to be injected, the total flipping time of the structure, the interval between flipping, the presence or absence of agents that promote cell adhesion (such as fibronectin or gelatin).
Initially, a cell density of $2.5 \cdot 10^6$ cells/ mL_{medium} was tested, but the number was too low so that even at the time of seeding they could not completely fill the channel; we then decided to drastically increase the cell density to $30 \cdot 10^6$ cells/ mL_{medium}, but in this case the amount of cells required was too high compared to the very small volume of culture medium they are suspended into. Therefore, the best option was to focus on $10 \cdot 10^6$ cells/ mL_{medium}, without the use of coating

agents. The use of different cell lines was also tested: initially only HUVECs were used and later MSCs were also added as support during endothelial cell proliferation [51]. Coculture of HUVECs and MSCs was done respecting a ratio of 70:30 of the two cell lines.

After injecting the cells, to prevent them from leaking out of the channel during the flipping hours, it is necessary to close the ends of the needles with integral closures. The flipping step is recommended to prevent the cells from settling only on one side of the channel due to the gravity effect. Before connecting the structure to the perfusion pump it is recommended to let the structure rest in the incubator overnight, renewing the medium inside the channel. A summary of the protocol used is listed below:

- bioprinting of the vascularized structure;
- cooling at 4°C for 5 min and wash-out of the Pluronic®;
- seeding of cells into the channel in density $10 \cdot 10^6$ cells/ mL_{medium};
- closing the needles with sterile integral cap;
- place in 37°C incubator and flip the structure of 180° every 30 minutes for 2 hours;
- renew the medium inside the channel
- leave overnight in incubator before connecting to perfusion pump.

A brief representation of the endothelialization steps can be seen in Figure 2.12 below:

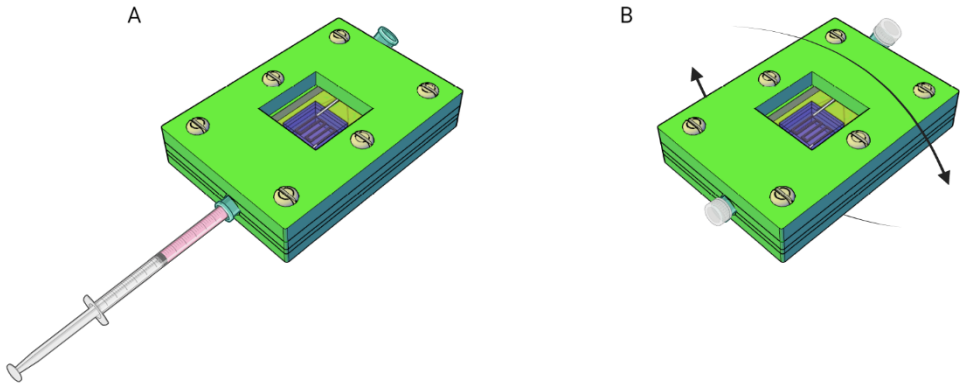

Figure 2.12: *endothelialization of vascular channel. Gently seed cells in the channel (A) and flip the structure to uniformly cover it (B).*

Perfusion Protocol

Once cell seeding within the channel has been done and after waiting overnight, we proceed by connecting the entire structure to a perfusion circuit. The purpose of perfusion is to continuously supply the medium to the cells, whether they are only lining the walls of the channel or encapsulated in the entire structure. Needles used in the seeding passage are kept inside the clamp and hoses are connected to their ends. Transfer and dosing of liquids in small quantities with high precision is controlled by a peristaltic pump, whose operating principle is based on moving fluid through tubes by compression and decompression. The pump clips are attached to the rotor, which spins and moves the fluid through the tubes; one works as an inlet and pushes the liquid into the structure, while the other act as an outlet and draws the liquid out. These mechanisms simulate the way our bodies pump blood, nutrients, and oxygen. Both hoses converge to the same reservoir that contains the culture medium, so there are no waste products. A schematic illustration of the setup can be seen in Figure 2.13.

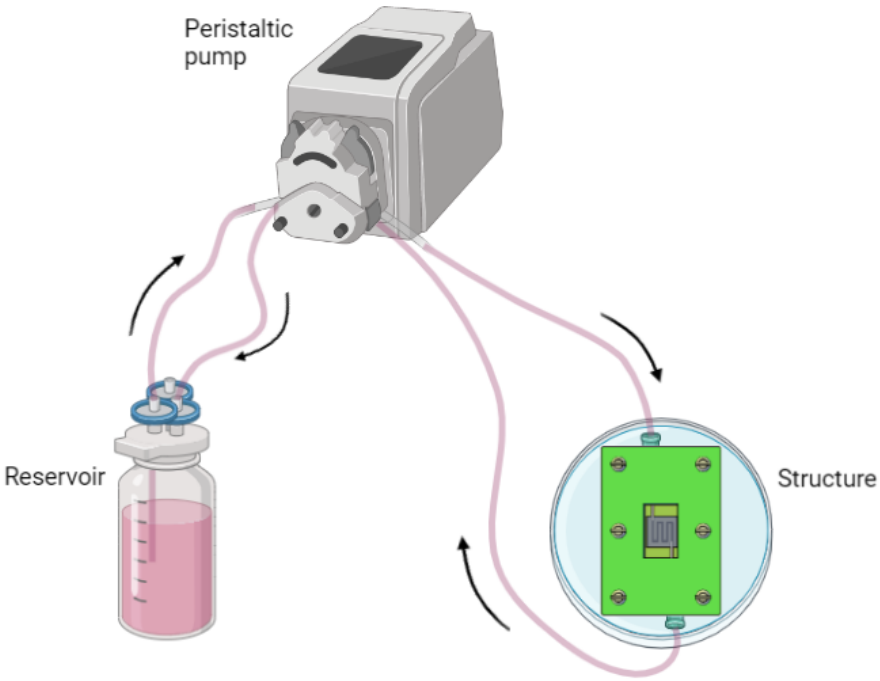

Figure 2.13*: schematic illustration of the perfusion setup.*

Even though the pumping system is completely sterile (the flexible tubes are autoclaved before being used), to limit the possibility of accidental contamination, a particular type of reservoir was chosen, as visible in Figure 2.14. Three 0.22 µm syringe filters were inserted into the cap of the reservoir to allow special membranes to remove particles and ensure the sterility of the liquid. One filter is used to connect the tube that draws the medium from the reservoir with those that allow the liquid to pass to the inlet needle; the second filter is used to sterilize the liquid that returns to the reservoir from the outlet tube; the third filter is the air one.

Figure 2.14*: reservoir with syringe filters. A) inlet filter; B) outlet filter; C) air filter.*

It is important to highlight that both the diameter of the tubes and the rotation value of the pump affect the flow rate, which if it is too high could go from laminar to turbulent and damage the channel and the entire structure, leading to failure of the experiment. By choosing the pump's rotational speed (rpm) and using the guidelines provided by the manufacturer, the flow rate can be determined: the peristaltic pump available in the laboratory (Dülabo PLP 380) has a speed range of 0.1-100 rpm, with an accuracy of 0.1 rpm, and is therefore capable of sustaining a flow rate between 0.03 and 30 mL/min as seen in Figure 2.15. For our experiments, the hoses have an internal diameter of 0.51 mm, and the chosen rotational speed is 0.5 rpm (equal to 10 µL/min) for the first day of perfusion, which is increased to 0.7 rpm (15 µL /min) for subsequent days of the experiment.

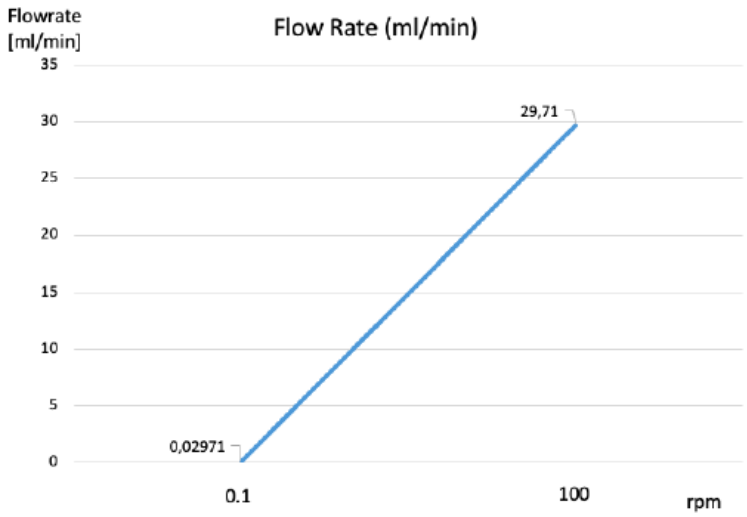

Figure 2.15*: calibration line of the Dülabo PLP 380 peristaltic pump. Conversion between rpm and flowrate (mL/min).*

2.3.4 CELL VIABILITY

An important aspect when conducting experiments with cells is to assess their viability. This term denotes the measurement of live, healthy cells in a population, comparing them with the number of dead ones. Considering cell viability is crucial as it can give important clues as to how the cells are within the chosen material, what their proliferation is, and what is the correct density to use. To do this a fluorescence analysis is used, which quickly gives an indication of the number of live and dead cells (and therefore called live and dead analysis): the materials used in this thesis are calcein acetoxymethyl ester (calcein-AM), propidium iodide (PI) and Hoechst 33258.

Calcein-AM is a dye that penetrates the cell membrane and is converted to calcein that is capable of complexing calcium ions, emitting green light when excited at the correct wavelength; PI is a fluorescent agent that is not membrane-permeable, so it is able to bind to the nucleic acids of dead cells (as their membrane is damaged) and emit red fluorescence when excited by light; finally, Hoechst is a popular nuclear counterstain that emits blue fluorescence when bound to dsDNA (double stranded DNA) of both live and dead cells nuclei.

Before performing the analysis, repeated washes of the structure with 1xPBS should be performed (3 times leaving for 5 min immersed) to completely remove cellular debris that may interfere with fluorescent dyes. If the structure under

examination is large, it is also recommended to cut it in such a way as to facilitate the entry of the fluorescent solution even in the deepest areas. Once the washes are done, immerse the structure in the solution prepared with the following proportions:

- 1:1000 calcein-AM;
- 1:500 Hoechst 33258;
- 1:250 propidium iodide.

This means that 1 µL of calcein-AM, 2 µL of hoechst and 4 µL of PI should be diluted in 1 mL of 1xPBS.
Once immersed, the structure is placed in an incubator for at least 45 minutes, making sure to cover it with tin foil to prevent light from deactivating the fluorophores.
After the time required for the dyes to penetrate inside the cells, it is necessary to remove the excess solution by washing with 1xPBS; this step is recommended to avoid overexposure and an unclear image once under the microscope.

2.3.5 FIXING AND STAINING

The method just described, *i.e.* Live/Dead analysis, has some substantial limitations: first, the analysis must be carried out very quickly, because there is a need for the cells to be alive for the fluorescent dyes to bind to them (at least for hoechst and calcein); second, there is the problem that the structure analyzed is in three dimensions. This leads to two key problems, the first is that analysis under an optical microscope is almost impossible because it is difficult to distinguish the different planes; the second is the thickness of the structure itself. Even when cutting it into smaller parts, the dyes poorly permeate to properly stain all cells.
One possible alternative solution is to use a different analysis technique that involves fixing the structure before staining it. In this way it is not strictly necessary for the cells to be alive to dye them; moreover, once the entire structure is fixed, it is possible to keep it stable for some time before looking at it under the microscope. However, to stain the cells once the whole construct is fixed, it is necessary to permeabilize the membranes to allow fluorescent molecules and/or

antibodies to penetrate. Permeabilization and membrane rupture causes cell death, thus not allowing to perform Live/Dead assays.
Paraformaldehyde (PFA) is generally used as a fixative: PFA is derived from formaldehyde dissolved in water or a buffer; its function is to crosslink cellular proteins by creating methylene bridges. A dilution in 1xPBS of PFA at 4% w/v is used in this thesis: after a few washes in 1xPBS, the structure is immersed in the PFA solution for at least 4 hours at 4°C. A non-ionic detergent, Triton X-100 diluted to 0.1% v/v in 1xPBS is then used to permeabilize the cell membranes. This solution is applied to the structure for about 5 min and then aspirated, all repeated about 3 times.
Finally, for the actual staining, phalloidin and DAPI were used at 1:200 and 1:800 dilutions, respectively. Phalloidin is a toxin capable of binding to F-actin filaments present in the cytoplasm and emitting a red/orange light when illuminated at the correct wavelength. DAPI (4',6-diamidin-2-phenylindole) is a dye that binds strongly to A-T rich regions in DNA to form a fluorescent blue complex and thus stains the nuclei. For this last part, immerse the structure in the solution containing both dyes for 1 hour at room temperature, after which aspirate and rinse with 1xPBS.

2.3.6 SECONDARY IMMUNOFLUORESCENCE

Immunofluorescence is a method used to detect the presence of specific antigens (usually proteins), whose known counterpart, *i.e.,* antibodies, is bound to a marker. The marker is a fluorophore, which is a dye that absorbs high-frequency waves and emits into the visible. There are two main immunofluorescence techniques: primary, or direct, and secondary, or indirect, which are schematized in Figure 2.16.
Primary immunofluorescence requires the antibody used to be directly coupled to fluorescent molecules; thus, the paratope of the primary antibody binds to the epitope of the antigen and light is emitted when excited. Secondary immunofluorescence is more complex and involves a two-step incubation process: first the primary antibody binds to the target epitope, then the fluorophore-labeled secondary antibody recognizes and binds to the primary antibody.

Secondary immunofluorescence was used in this thesis because, although more elaborate, it is more advantageous. In fact, to each "naked" primary antibody, bound to the fixed antigen, multiple labeled secondary antibodies can be bound, resulting in a brightness amplification.
E-cadherin, vimentin, CD31 and CD144 were used as primary antibodies. Briefly, E-cadherin is a calcium-dependent cell-cell adhesion molecule with pivotal roles in epithelial cell behavior (epithelial cells are rich in cell-cell junctions) and tissue formation; vimentin recognizes the intermediate filaments of the cytoskeleton of all cells; CD31 marks endothelial cells and is effective for vessel marking in angiogenesis; finally, CD144 recognizes a calcium-independent extracellular epitope, *i.e.* an adhesion molecule expressed on endothelial cells.
Compared with the fixing and staining protocol seen previously, an additional blocking step must be performed before adding the primary antibodies. Blocking consists of using a protein-rich solution (blocking solution, BS) that does not have binding affinity for the target antigen and reduces nonspecific binding while improving the signal-to-noise ratio of the assay by diminishing background interference. In this thesis, 1% BSA (Bovine Serum Albumin) + 0.1% Triton was chosen as blocking solution which is applied to cells for 4 hours at room temperature. After aspirating BS and doing washes with PBS-T (meaning 1xPBS with 0.1% Triton) add primary antibodies, diluted in blocking solution in this way:

- E-cadherin 1:50;
- Vimentin 1:100;
- CD31 and CD144 both 1:100;

Incubation with primary antibodies is performed at 4°C for 24 hours. Next, after overnight incubation with PBS-T+BSA 0.5%, the secondary antibodies are added for 8 hours at room temperature in the dark. All the secondary antibodies are diluted in blocking solution in 1:1000 concentration. After a wash in PBS-T, samples are left overnight in PBS-T+BSA 0.5%; other dyes can be added the next day if necessary (such as phalloidin and DAPI seen in the fixing and staining protocol). Finally wash everything with 1xPBS.

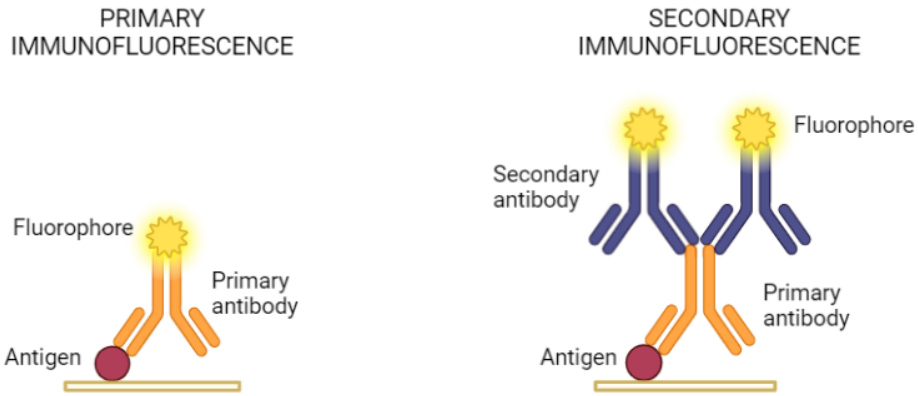

Figure 2.16*: schematic illustration of primary (direct) and secondary (indirect) immunofluorescence.*

2.3.7 ANGIOGENESIS ANALYZER

Angiogenesis assays based on in vitro capillary-like growth of endothelial cells (EC) are widely used to compare the functional capacities of various types of EC and progenitor cells. Angiogenesis is defined as the growth of new blood vessels from pre-existing ones; it is a complex and critical process that takes place during vertebrate development, in specific physiological conditions in adult individuals and during different pathologies like tumor. Accurate and objective evaluation of these phenomena is necessary for the full comprehension of this process. Most in vitro angiogenesis models were designed based on the so-called "sprouting angiogenesis" differentiation process, whereby pseudo-capillary formation mimics several steps of the *de novo* angiogenesis. To do so, we used a simple and precise tool built in the *ImageJ* environment. The "Angiogenesis Analyzer" program has been used to extract characteristic points and elements of endothelial cells network. This image analysis software was successfully applied to characterize meshed and/or branched structures. Once the image of interest is processed, the automatic analysis conducted produces a set of results consisting in a group of vectorial objects, like node, junction, segment, branch and mesh [52].

Chapter 3
EXPERIMENTAL RESULTS

In this chapter we will present the main experimental results obtained, focusing first on the choices of the best hydrogel printing conditions, followed by a section devoted to structure printing tests with the serpentine inside the created clamp. Finally, the endothelialization tests and cell analyses perfusion are presented.

3.1 HYDROGELS PRINTING

The previous chapters listed the general characteristics of the hydrogels that were used for the development of this thesis, GelMA and Pluronic®. This section will show the results of printing tests of the materials that led to the decision to use certain specific parameters during the experiments.

3.1.1 GelMA PRINTING PARAMETERS

As mentioned in Section 2.2.2, GelMA is a material whose printing is highly dependent on the chosen temperature. Keeping the type of nozzle constant, a 25G metal straight-tip, different printing results were analyzed by varying the temperature between 20°C and 28°C with 4°C increments. The 25G nozzle was chosen from previous studies conducted in the laboratory, highlighting that acellular GelMA printing with the metal straight-tip turns out to be more accurate when compared to the same printing using the 25G conical-tip.

The results, reported in Figure 3.1, show that the optimal printing temperature is 23.5°C$\pm$1.0 as the desired shape is properly maintained. It is immediate to see that at lower temperatures a more granular print is obtained, due to the GelMA having gelled too much and created numerous intermolecular bonds that increase viscosity. In contrast, for higher temperatures, the material appears as too liquid and the print is inconsistent with total loss of details.

In addition, the printing pressure for GelMA at 20°C is too high, about 340 kPa, a value that would induce severe cell death when printing cell-embedded gels. On the other hand, the printing pressure for 28°C was set at the lowest limit to achieve material leakage, with a pressure around 20 kPa. The inverse

proportionality between temperature and pressure is clear: as the first increases, the second decreases.

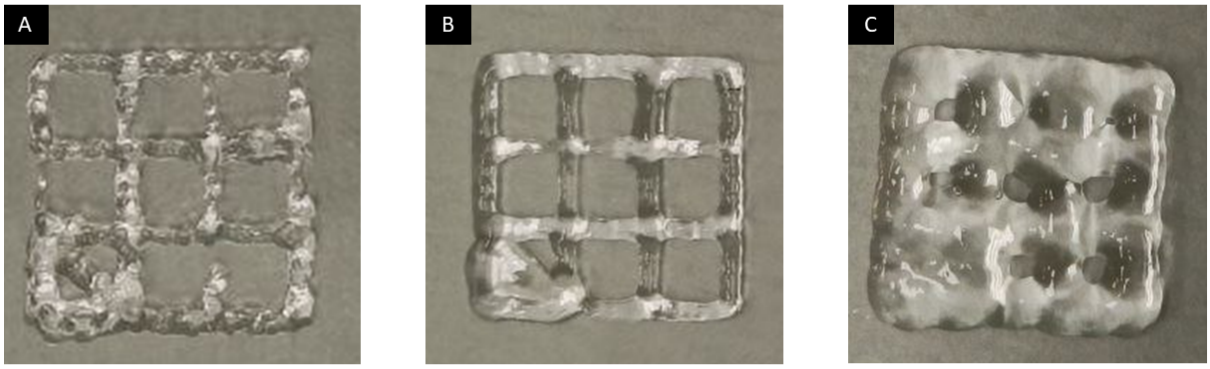

Figure 3.1*: GelMA printed at A) 20°C and 340 kPa, B) 24°C and 60 kPa, C) 28°C and 20 kPa.*

We also analyzed the correct infill percentage of the print in GelMA structure. To do so, two layers of a square were printed with 40%, 60%, 80% and 100% infill and a qualitative analysis was done. Printing was done using a 25G straight-tip nozzle, keeping the temperature constant at 24°C and the pressure at 70 kPa. As visible in Figure 3.2, 40% is to be excluded because the print is not cohesive, there are too many gaps, and sometimes the second layer fails to adhere properly to the first. 60% was also ruled out because of too many gaps present, which would cause medium to leak from the material once connected to the peristaltic pump. 100% was eliminated because, conversely, the filling is too dense and the printing process would become too heavy and time-consuming, erasing the advantages of choosing multi-material extrusion bioprinting. Also, the fully filled structure appears thicker and more rounded than desired, increasing the risk that during the printing process the overlying layer will be printed inside the one already deposited. For this thesis, the choice was to print the structure with 80% fill, which succeeds in properly balancing accurate and well-structured printing.

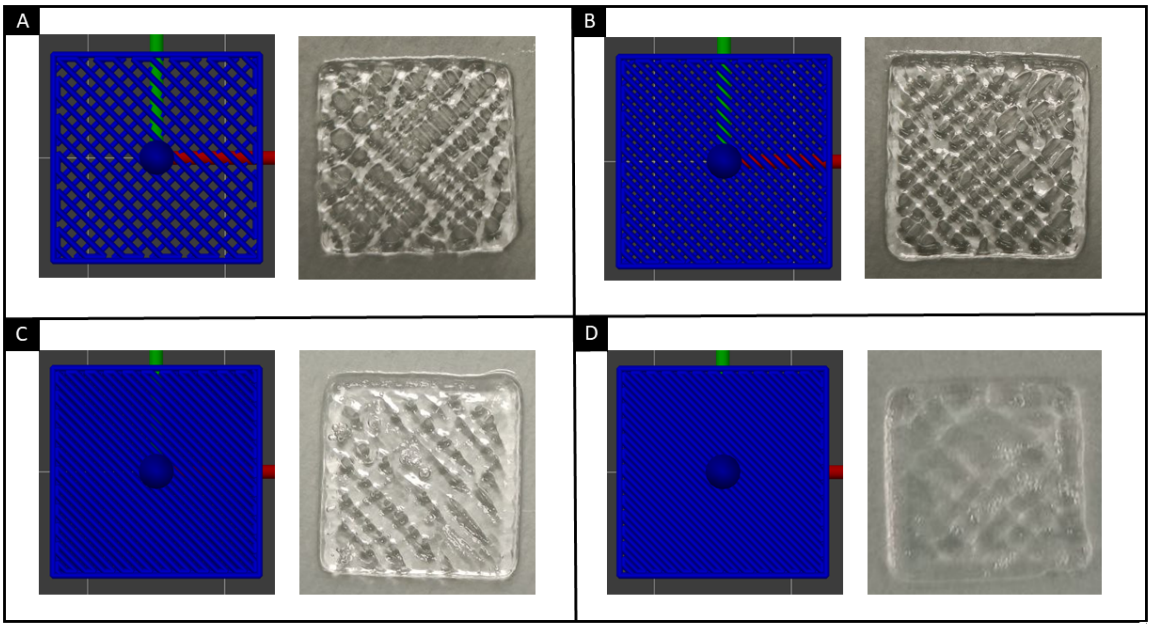

Figure 3.2*: GelMA printed with different filling percentage: A) 40%, B) 60%, C) 80%, D) 100%.*

3.1.2 PLURONIC® PRINTING PARAMETERS

Pluronic® at room temperature is a viscous gel, so the only choices that can be made regarding printing refer to the diameter of the needle used and the related printing pressure. With the aim of creating a perfusable channel, in the multi-material bioprinting process the focus for printing the Pluronic® was on the use of two metal straight-tip nozzle, 25G or 27G, with internal diameters of 0.25 mm and 0.21 mm, respectively.

To evaluate the correct printing pressure range of the Pluronic®, the diameters obtained from material printing tests were measured for a pressure ranging from 300 kPa to 600 kPa with 50 kPa increments (performed for the two different needle sizes). The upper limit was set at 600 kPa since this is the maximum pressure the compressor can supply to the printer, while the lower limit was chosen since below 300 kPa even the 25G needle cannot extrude a continuous filament. For simplicity, we chose to print a single filament of Pluronic® (having the same design thickness as the serpentine) and, after capturing the images under a microscope with a 4x objective, they have been analyzed using *ImageJ* software to determine the diameters.

Table 3.1 and Figure 3.3 shows the average channel size while Figure 3.4 shows the evolution of the diameters at the respective printing pressures.

Table 3.1*: Pluronic® printing pressure and channel size for 25G and 27G nozzles*

	AVERAGE DIAMETER ± STANDARD DEVIATION	
PRESSURE	**25G (0.25 mm)**	**27G (0.21 mm)**
300 kPa	0.1915 ± 0.0111	NaN
350 kPa	0.2724 ± 0.0143	0.1542 ± 0.0112
400 kPa	0.6208 ± 0.0463	0.1952 ± 0.0111
450 kPa	0.7971 ± 0.0604	0.2373 ± 0.0103
500 kPa	1.2560 ± 0.0578	0.3106 ± 0.0112
550 kPa	1.5048 ± 0.0574	0.3525 ± 0.0212
600 kPa	1.9956 ± 0.0757	0.3852 ± 0.0173

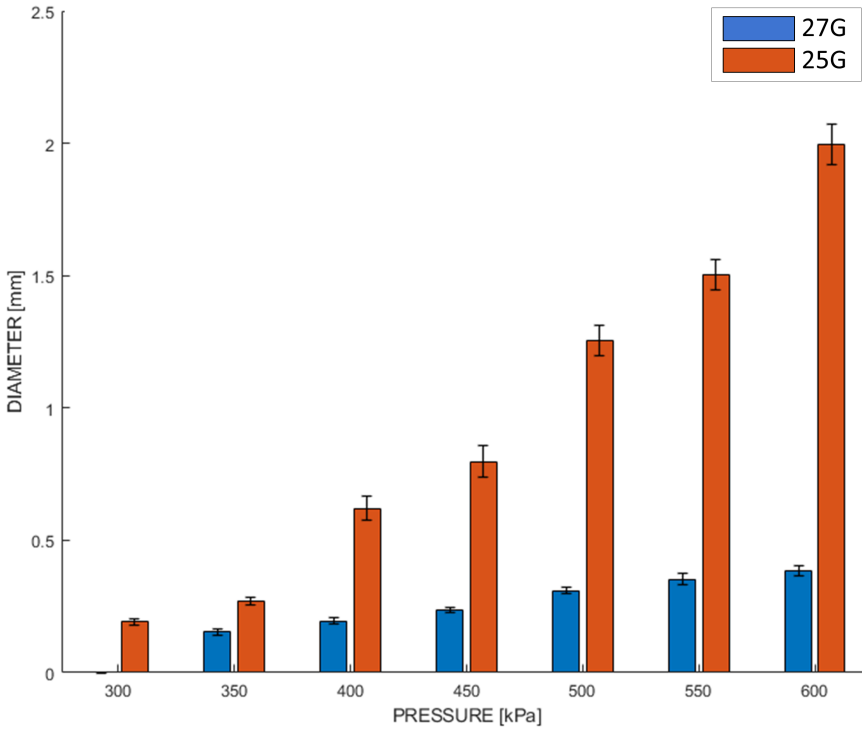

Figure 3.3*: Pluronic® channel size for 25G and 27G nozzles at different pressure.*

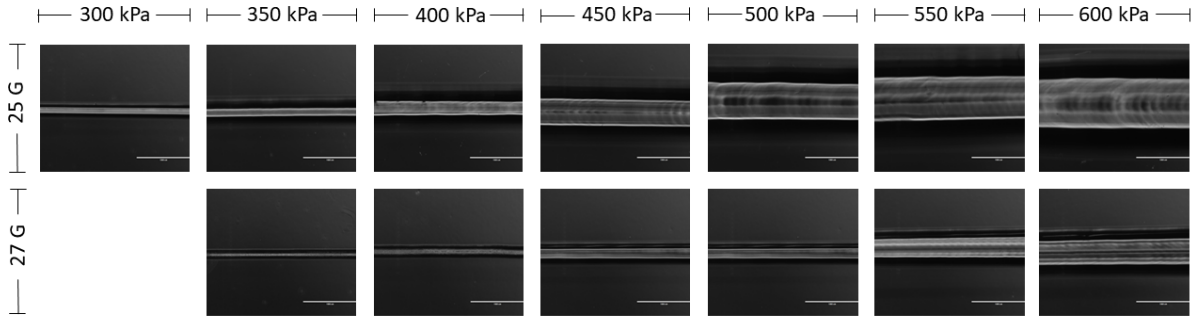

Figure 3.4*: evolution of Pluronic® diameters at different printing pressures.*

Considering that the design measurements of the GelMA contour layer visible in Figure 3.5 have a containment width of 0.9 mm, we opt to print the Pluronic® with the 25G nozzle at a pressure between 400 kPa and 450 kPa. To avoid the material from filling all the available space and to prevent subsequent GelMA layers from ruining the channel print, a pressure of 410 kPa was chosen.

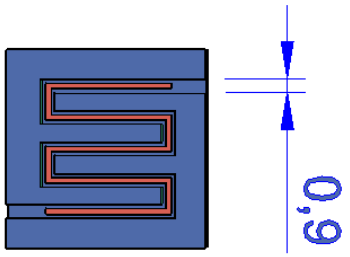

Figure 3.5: *size of GelMA contour layer.*

3.1.3 PRINTED STRUCTURE AND PERFUSION CIRCUIT

Once the conditions and printing parameters for the different hydrogels have been fixed, various trials are conducted to optimize the multi-material bioprinting process of the proposed structure. Several attempts were made to optimize the calibration of both cartridges at the same point such that, when printing the Pluronic®, it starts exactly inside the created guidelines. Figure 3.6 shows the result obtained at the end of printing inside the designed clamp. The printing was performed using a 25G straight-tip nozzle for both GelMA and Pluronic®, setting a temperature for GelMA of 24°C and a pressure of 60kPa, while for Pluronic® a pressure of 410 kPa. It is useful to remember, however, that the multi-material

printing process is advantageous because it allows high repeatability of the test, but it is still subject to parameters that vary within specific ranges. The picture shows a printing attempt carried out under non-sterile conditions, so the Pluronic® was colored red to facilitate visualization. After UV light exposure and covering with PDMS, the closed clamp is placed in the refrigerator at a temperature of 4°C for about 5 min to liquify the Pluronic®. At this point a wash-out is performed to completely remove the residual material: this was done using two 0.25 mm (25G) diameter flexible-tipped needles (from Drifton) and cold 1xPBS also stained red, so that the flow of liquid inside the serpentine could be seen (Figure 3.6-B).

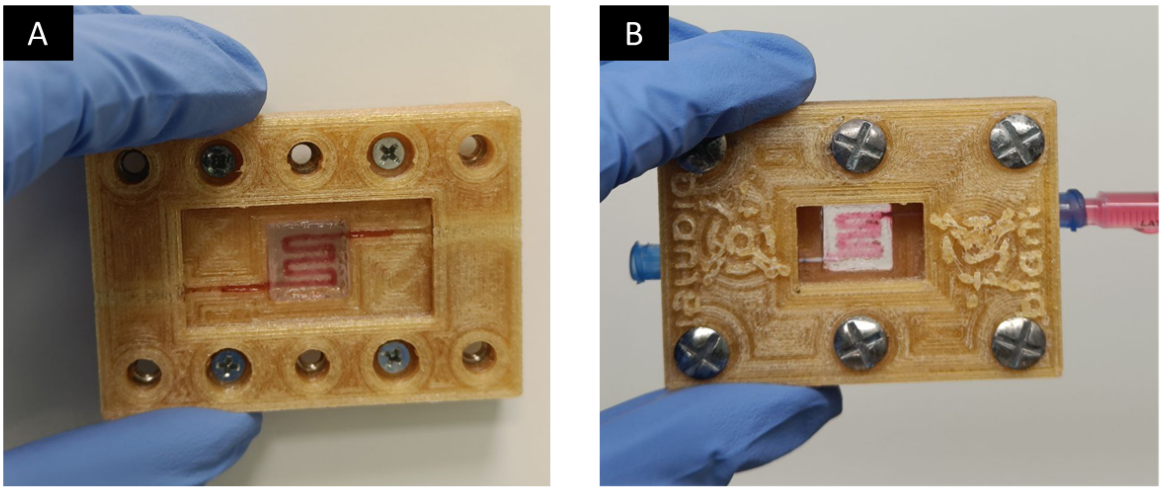

Figure 3.6*: A) Printed structure inside the clamp; B) structure after Pluronic® wash-out.*

The entire structure could then be connected to the perfusion circuit to assess whether the pump was working properly and if the various connections between the hoses and the reservoir filters were accurate. Perfusion tests were performed by keeping the same needles used for the previous wash-out inside the clamp and connecting the hoses to them via specific plugs. In this way, the peristaltic pump can constantly flow the liquid inside the created empty channel.

To replicate the experimental setup shown paragraph 2.3.3, the peristaltic pump (Dülabo PLP 380) was equipped with two hoses with internal diameter of 0.51 mm (from Cole-Parmer); for the reservoir, three LLG-Syringe Filters with 0.22 µm pore size and two colder luer fitting male (from Drifton) were used to connect the inlet and outlet hose to the corresponding filter. For the various attempts, the reservoir

was filled with red-stained 1xPBS so that the passage through the serpentine and the hoses could be easily seen. The actual setup is shown in Figure 3.7.

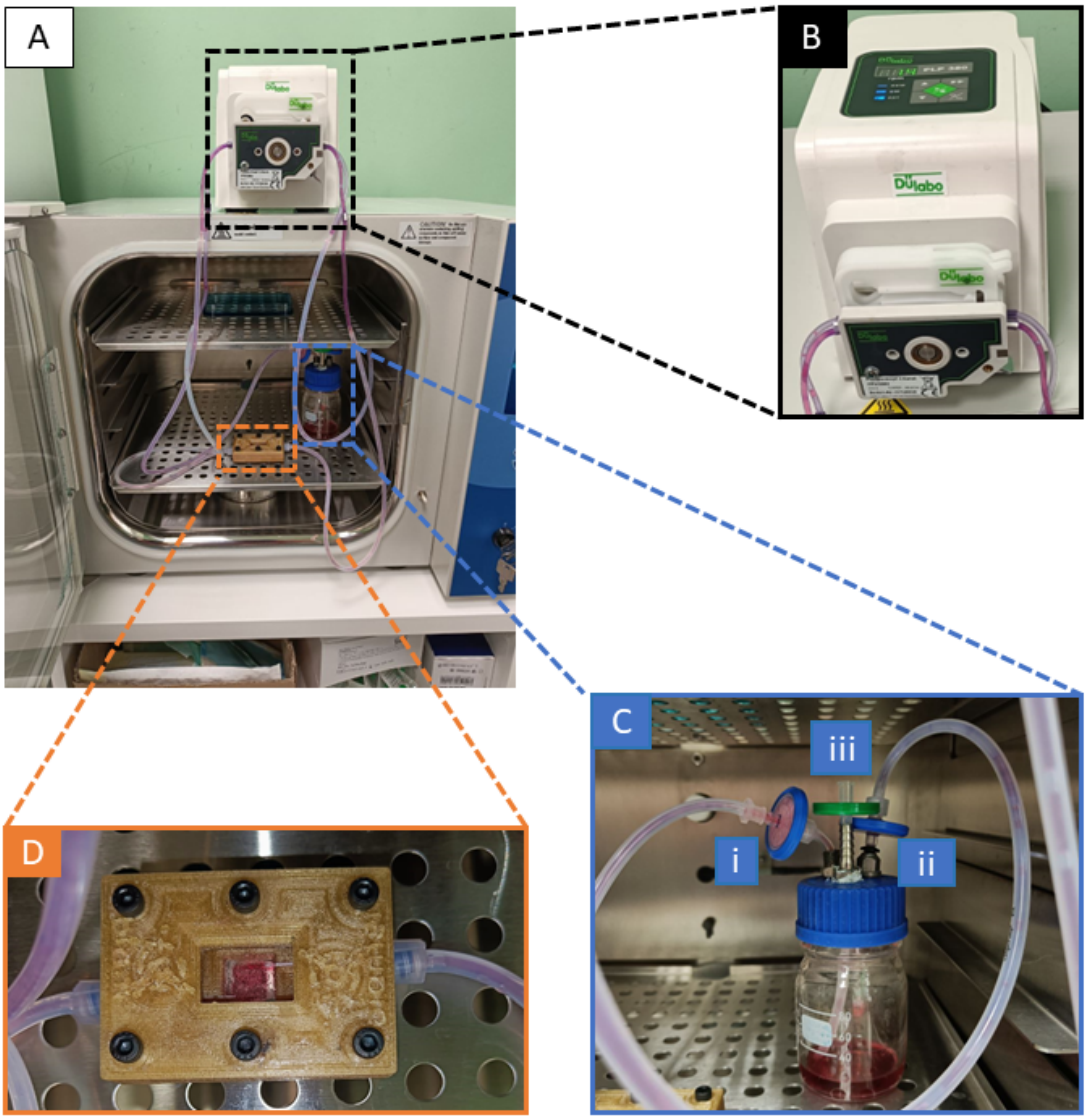

Figure 3.7*: A) perfusion setup. B) Peristaltic Pump Dülabo PLP 380. C) Reservoir setup with 0.22 µm filters and hoses with internal diameter of 2.6 mm: i) input side; ii) output side; iii) air filter. D) Zoom on the printed structure in perfusion: 22G flexible-tip needles and colder luer fitting male attached to hoses.*

3.2 CELLULAR TESTS

In this section, the most significant results obtained in the biological experiments performed will be illustrated. First the interaction of the chosen cell lines with GelMA will be explored in depth, and then the endothelialization tests will be shown.

3.2.1 CELL VIABILITY FOR HUVEC AND MSC

We investigated cocultures of mesenchymal stem cells (MSCs) and endothelial cells (HUVEC). The main reason for choosing to use these two cell lines is that, as shown in the literature, MSCs act as a support for HUVECs, promoting endothelialization and angiogenesis [51]. Before analyzing the crosstalk between these two cell types and evaluating if HUVEC could modulate the phenotype and proliferation of MSCs, cell viability tests are performed to assess and evaluate how cells behave when embedded in the chosen hydrogel. 70% HUVECs and 30% MSCs in $5 \cdot 10^6$ cells/mL_{medium} concentration are mixed in a 1:25 ratio with GelMA: 100 µL of the cellularized GelMA are cast into a PDMS mold to obtain small discs. After being cross-linked with UV light, they are placed inside multiwell plates and cultured half with HUVEC medium only and the other half with 50% HUVEC and 50% MSC medium. The choice to culture distinctly with two different mediums was made to assess the difference in cell viability and morphology according to the culture environment in which cells live.

The viability of the cells encapsulated in the hydrogel and statically cultured is investigated using Live/Dead fluorescence assay previously explained in Section 2.3.4: the assay is performed at day 2, 7, and 14, and the results are summarized in Figure 3.8 and Figure 3.9. As shown, it can be concluded that in terms of cell viability, there are no significant differences between GelMA and cells discs cultured in full HUVEC medium and half-and-half medium. Data were analyzed using a MATLAB program, exploiting One Way ANOVA analysis to calculate p-values by comparing viability at same days and different culture medium. The p-values were greater than 0.05 so they were not included in the graph as not significant. P-values greater than 0.05, in fact, indicate that the experimental difference is not statistically meaningful, so the results are comparable with each other.

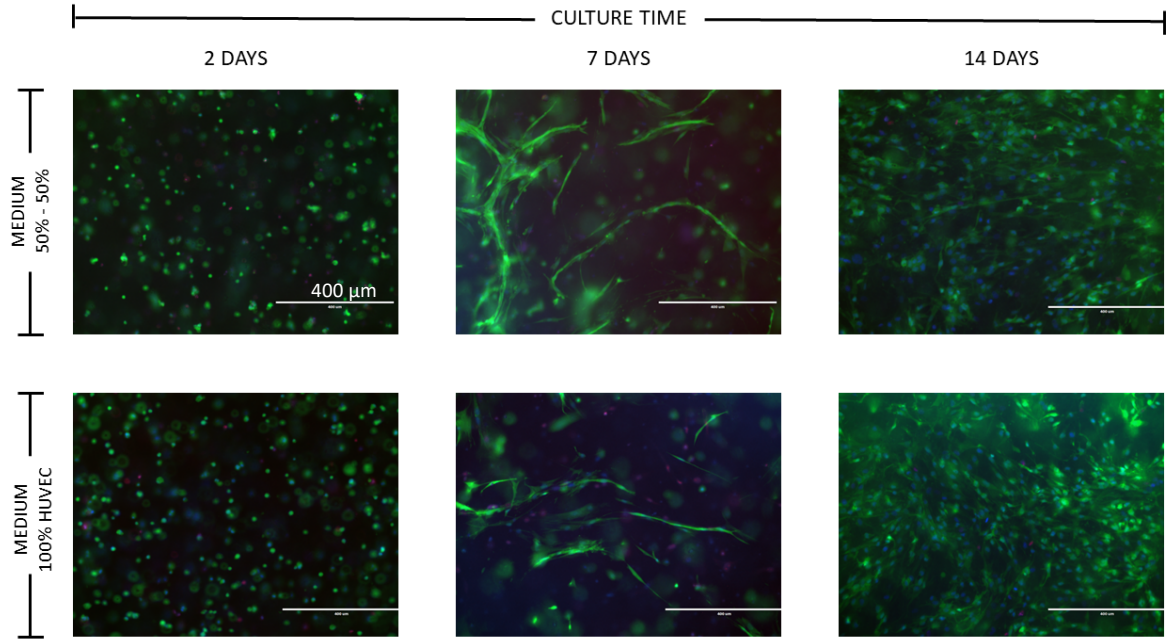

Figure 3.8: *Live/Dead fluorescence assay made at days 2, 7 and 14 in GelMA embedded with HUVECs + MSCs and statically cultured using 50% HUVEC - 50% MSC and only HUVEC medium. Fluorescence is obtained using Hoechst (blue), calcein-AM (green) and propidium iodide (red). Scalebar is 400 µm.*

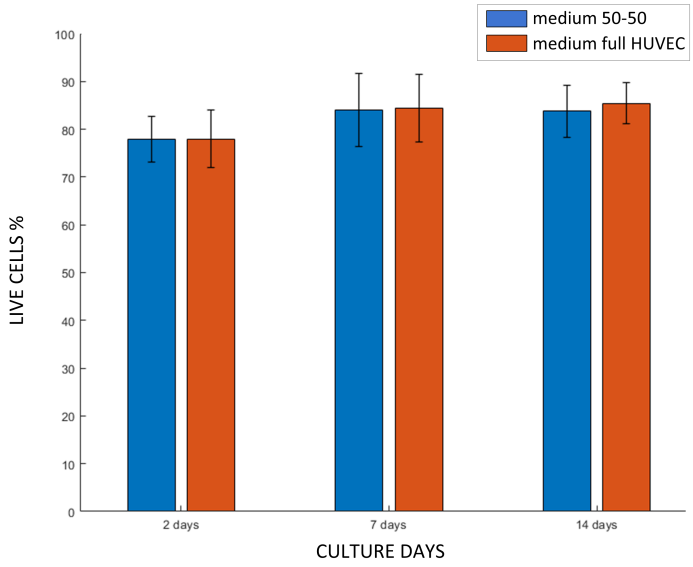

Figure 3.9: *MATLAB graph representing cell viability % ± standard deviation of HUVEC + MSC embedded in GelMA on different days of culture. As per the legend in blue are represented samples cultured with 50% HUVEC - 50% MSC medium while in orange are those cultured with 100% HUVEC medium. Experimental difference among samples analysed at the same day is not statistically meaningful.*

Both conditions analyzed show that cell viability increases with culture time, as can be seen in Figure 3.10, indicating that cells are in a favorable environment for

proliferation and differentiation. One Way ANOVA test was done to validate this claim: cell viability of samples cultured with HUVEC medium at day 2 and 14 was compared, and the same thing was done for samples cultured with 50-50 medium. In both cases, the p-value obtained is less than 0.05 highlighting how over the days the number of cells increased.

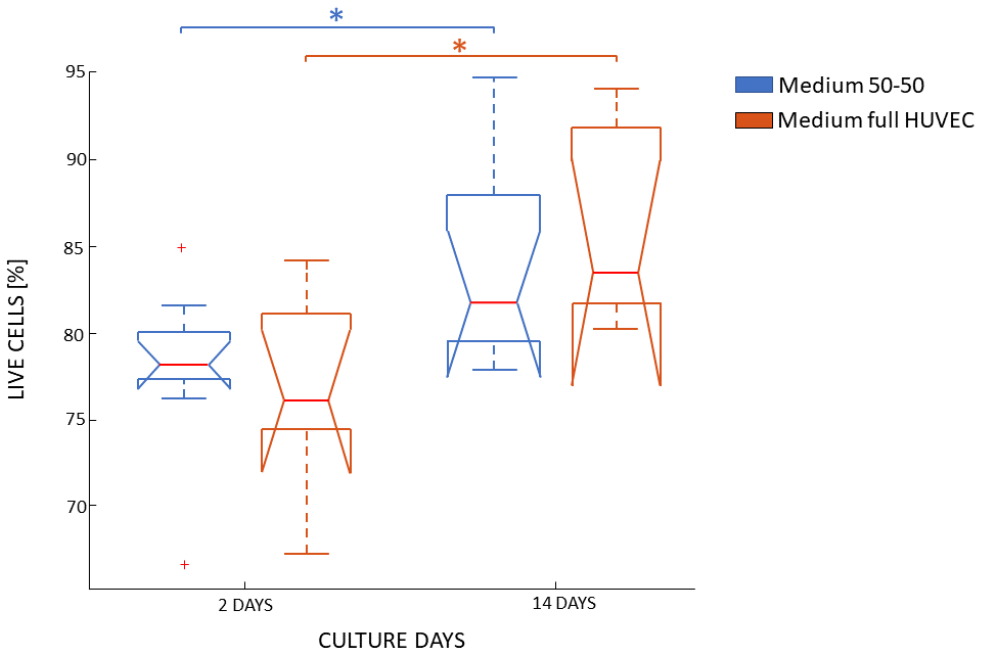

Figure 3.10*: One Way ANOVA test: increased cell viability over the 14 days of static culture (*p < 0.05).*

Another goal of the synergistic study of the HUVECs and MSCs coculture system is to evaluate how the presence of endothelial cells affect the differentiation status of mesenchymal stem cells and vice versa. Again, samples with cells embedded in GelMA were statically cultured half in 50% HUVEC - 50% MSC medium and the other half with 100% HUVEC medium. To analyze how this affects the phenotype and morphology of the cells involved, we did an immunofluorescence analysis using the procedure explained in section 2.3.6. Images were acquired through a confocal microscope (ZEISS LSM 800) and processing was done using a particular *ImageJ* software tool called 'Angiogenesis Analyzer'. This allows analysis of cellular networks; typically, it can detect and analyze the pseudo vascular organization of endothelial cells embedded in gels. The results of this part of the analysis were

obtained using the CD31 antibody that binds only HUVEC cells. No statistical significance was evident between filament length (also called sprout length) measured on days 2, 7, 14 and 21 between samples treated with HUVEC medium only and those treated with half-and-half medium. Therefore, only the analyses performed in the samples with fully endothelial culture media at day 21 were shown in Figure 3.11.

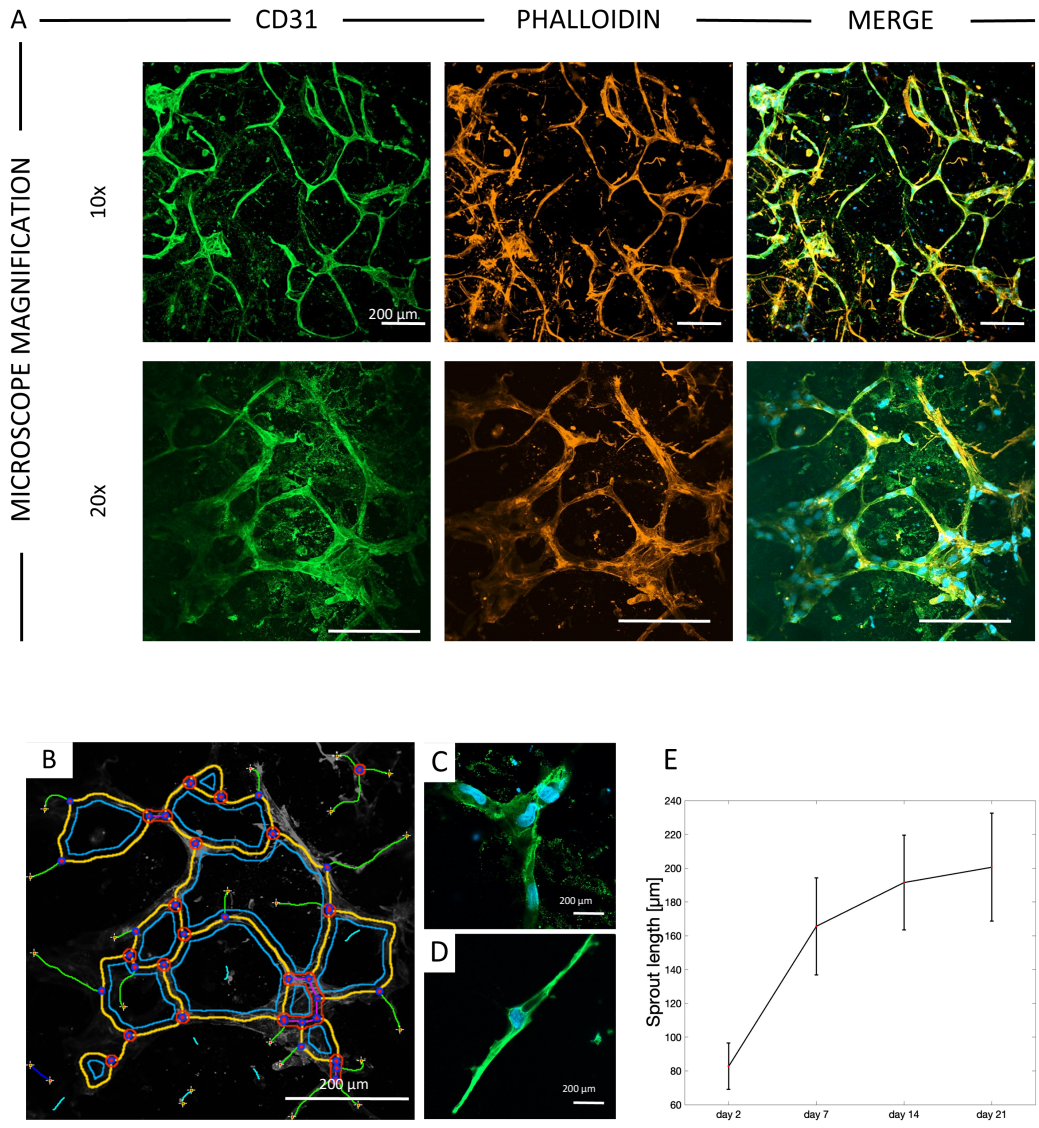

Figure 3.11: *HUVECs and MSCs coculture at day 21 (70%-30%, 5·10^6 cells/mL) using full HUVEC medium. A) Qualitative morphology analysis using CD31, phalloidin and DAPI. B) Image obtained using the 'Angiogenesis Analyzer' plugin of ImageJ software. Nodes, branches and meshes are highlighted. Scalebar 200 µm. C) Cell junction. D) Single cell elongation. E) Sprout length increase during the 21 days of culture. Filament length is obtained by calculating the nucleus-nucleus distance.*

The last set of immunofluorescence tests involves image analysis using E-cadherin antibody that indicates endothelial mesenchymal transition. By analyzing the intensity of the emitted signal, shown in Figure 3.12, the amount of endothelial component is assessed in a qualitative way. The results confirmed what we expected: in the 100% HUVEC culture medium, the signal is brighter, highlighting that without MSCs nutrients, the differentiation of mesenchymal to endothelial is encouraged. Taken together, these results led us to draw two important conclusions: first, cells embedded in GelMA are viable and proliferate over time, and second, culture with only HUVEC medium incentivizes the differentiation of MSCs into endothelial.

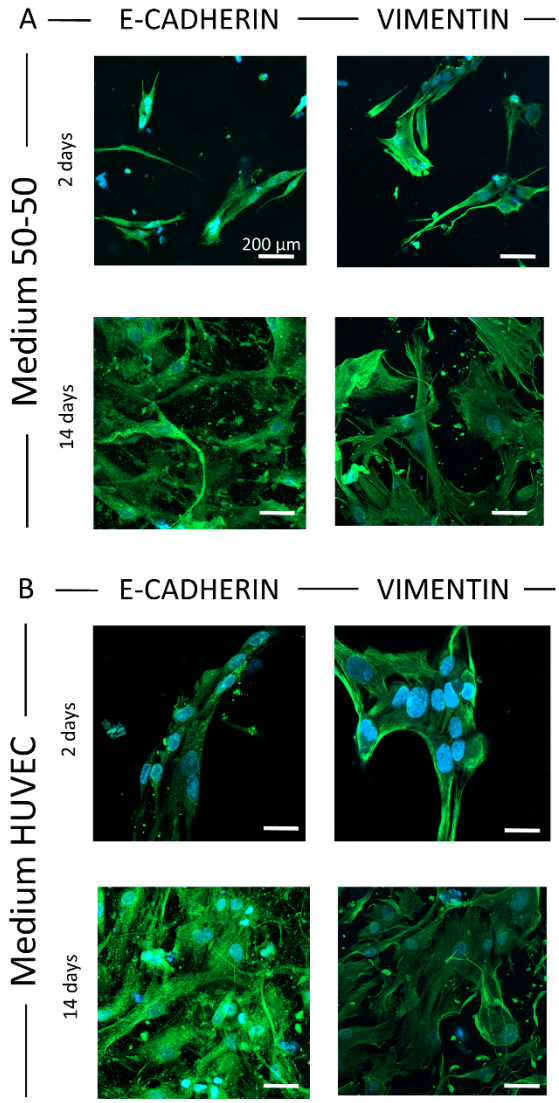

Figure 3.12: *HUVECs and MSCs coculture (70%-30%, $5 \cdot 10^6$ cells/mL) using A) medium 50% HUVEC – 50% MSC and B) full medium HUVEC. Immunofluorescence analysis using E-Cadherin and Vimentin at day 2 and day 14 for both cultures. Scalebar 200 µm.*

3.2.2 ENDOTHELIALIZATION TRIALS

Endothelialization tests were performed following the method listed in section 2.3.3. Table 3.2 summarized all the tests performed, highlighting the major differences among them. All experiments were performed with the multi-material bioprinting technique shown in section 2.2.3, and following the conclusions drawn in the previous paragraph, the perfusion step was done by filling the reservoir with HUVEC medium only.

Table 3.2*: list of endothelialization trials*

Experiment	Cell density	Proportion HUVEC+MSC	Culture days
1	$2.5 \cdot 10^6$ cells/mL	100%	FAILED
2	$30 \cdot 10^6$ cells/mL	80% + 20%	FAILED
3	$10 \cdot 10^6$ cells/mL	60% + 40%	FAILED
4	$10 \cdot 10^6$ cells/mL	70% + 30%	3
5	$10 \cdot 10^6$ cells/mL	70% + 30%	3
6	$10 \cdot 10^6$ cells/mL	70% + 30%	7
7	$10 \cdot 10^6$ cells/mL	70% + 30%	7
8	$10 \cdot 10^6$ cells/mL	70% + 30%	14

Some initial experiments failed because the endothelialization protocol had not yet been properly defined. In fact, initially a cell density of $2.5 \cdot 10^6$ cells/mL_{medium} HUVEC was used, which resulted to be too low to completely fill the channel and recreate a cohesive vascular structure. The next attempt was made by greatly increasing the cell density using both HUVEC and MSC, but in this case, it was too high: the number of cells required was too much compared to the small space in which they were placed, so many did not adhere to the GelMA-printed structure and were washed out with the flowing of medium during perfusion. The next attempt was made using an intermediate density, $10 \cdot 10^6$ cells/mL_{medium}.
Initially a ratio of 60% HUVEC and 40% MSC was chosen, and led to the conclusion that the number of mesenchymal stem cells was too high. The choice therefore fell to using 70% HUVEC and 30% MSC, leading to promising results already after 3 days of perfusion. Figure 3.13 shows the structure 1 day after seeding the cells into the empty channel.

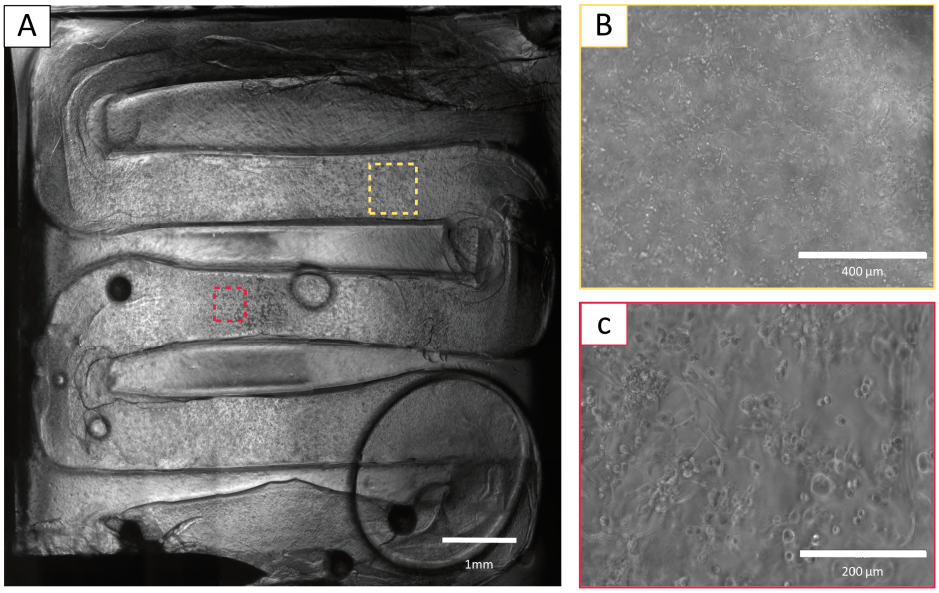

Figure 3.13*: seeding of HUVEC and MSC (70% - 30%, 10·10^6 cells/mL) inside the printed serpentine (A). Zoom on cells to assess shape after the first day in static conditions: scalebar 400 µm (B) and 200 µm(C).*

To further optimize the protocol and determine the ideal attachment time of cells to GelMA, we fine-tuned the flipping of the constructs. In experiment 1, the structure was flipped immediately after seeding 180° for two hours, and flipped back to the initial position for another two hours. After this, the structure was connected to the perfusion circuit. In the second and third experiments, the structure was rotated 90° every 15 minutes for a total of 4 hours, and then connected to the perfusion circuit. From the fourth trial, we chose to turn the structure 180° every 30 minutes for a total of 4 hours and let it sit overnight – with the renewed medium - before connecting it to the perfusion circuit. In this way, we avoid stressing the cells with flow shortly after being placed inside the channel, and thus avoid detaching them if not yet well adhered to the GelMA. Also, from the sixth experiment onward, we chose to increase the flow rate from 0.5 rpm to 0.7 rpm after the first day of perfusion.

Figure 3.14 shows the results obtained after 1, 3 and 7 days of perfusion with the optimized protocol (70% HUVECs and 30% MSCs using a cell density of $10 \cdot 10^6$ cells/mL$_{medium}$). At the chosen timepoints, the structures were disconnected from the circuit, fixed following the protocol explained in section 2.3.5, and stained using phalloidin (in red, binds to cytoplasm) and DAPI (in blue, binds to nuclei). The images, acquired by confocal microscope show that even after only one day

of perfusion, cells start elongating, and create a compact and uniform network after 7 days of perfused culture.

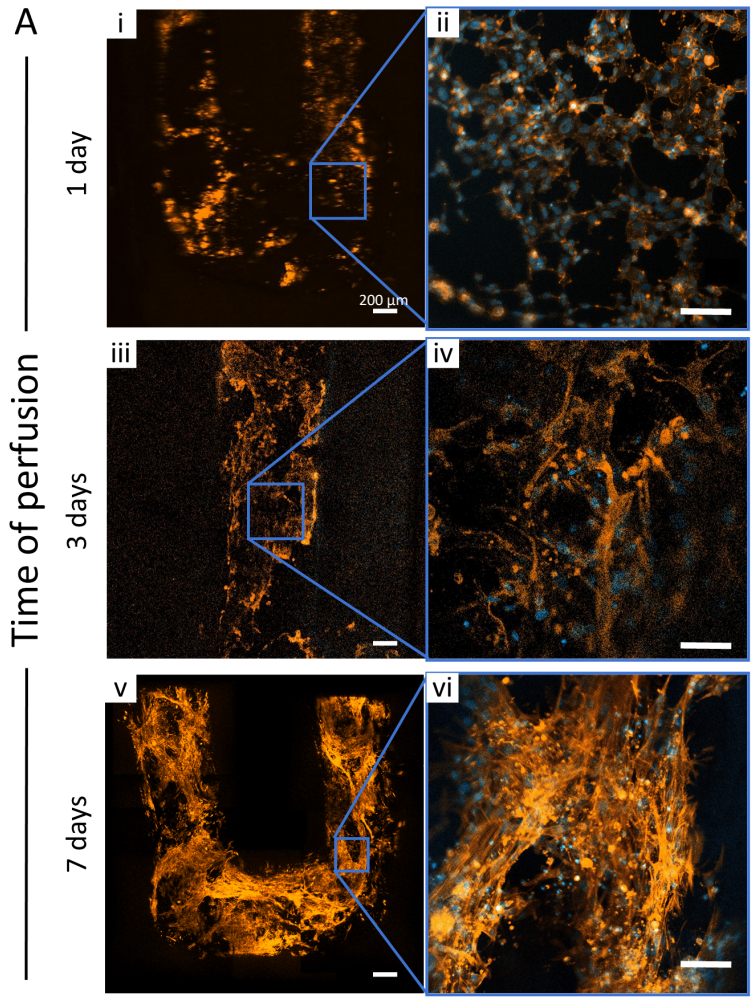

Figure 3.14: *A) HUVEC and MSC (70% to 30%, 10·10⁶ cells/mL) inside the serpentine analysed with confocal microscopy after 1, 3 and 7 days of perfusion. In red phalloidin, in blue DAPI. Initially cells are roundish (i,ii) and acquire an elongated morphology due to shear stress generated by the medium under perfusion (v,vi). Scalebar 200 µm.*

The best results were obtained after 14-days of continuous perfusion. As can be seen in Figure 3.15, we obtained an almost perfect channel: by exploiting the orthogonal projection in the XZ axes, possible thanks to the acquisition of different planes in succession (call z-stack) at confocal microscope, we can see the lumen contained between the endothelial walls. In biology, lumen defines a cavity anatomically bound by the complex of tissues that constitute the organ cavity, in our case the blood vessel.

In the previous analyses carried out mainly at day 7, the lumen was not fully formed, and the network of cells mainly covered the lower half of the structure, *i.e.* the one to which, by force of gravity, more cells had adhered.

For day 14 analyses we also used the CD31 antibody, together with DAPI and phalloidin, to visually assess the obtained endothelialization state.

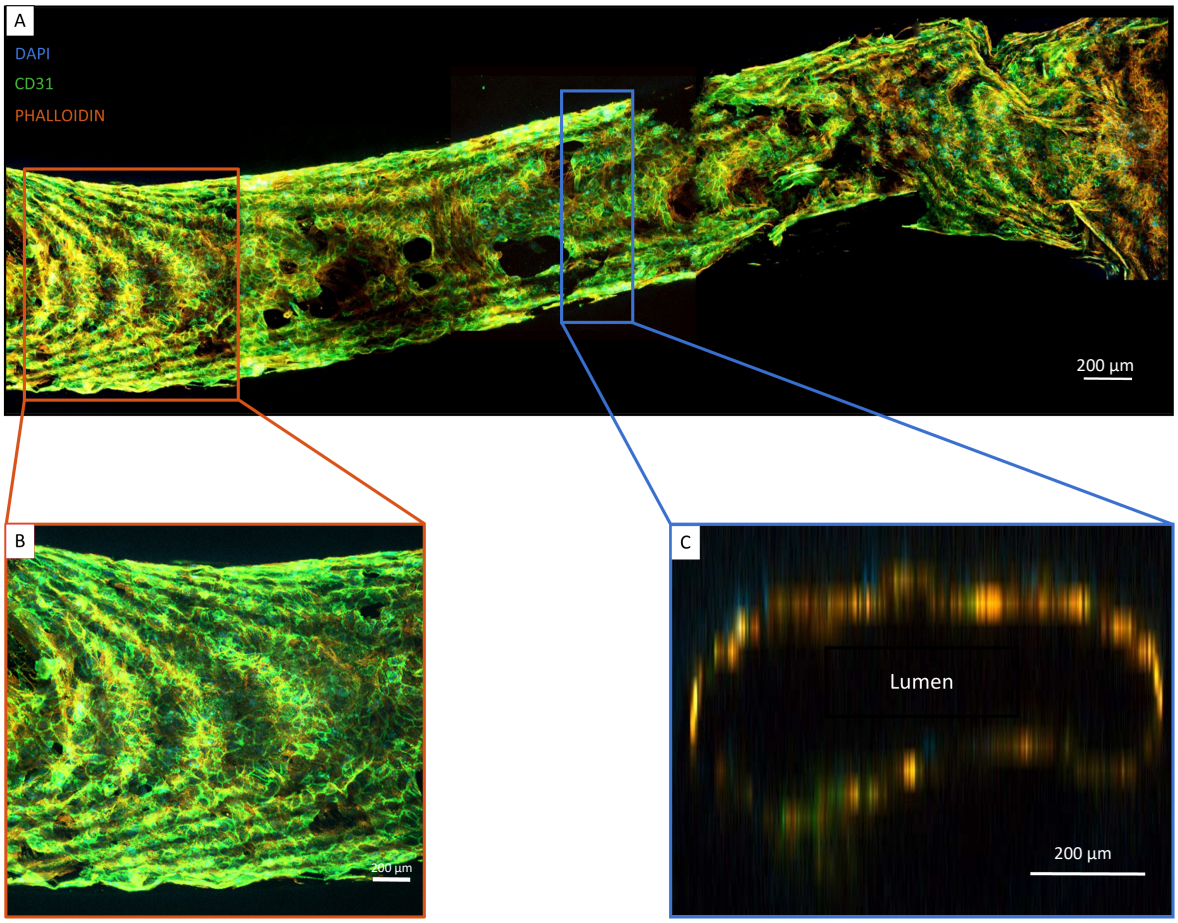

Figure 3.15*: A) HUVEC and MSC (70% to 30%, 10·10⁶ cells/mL) inside the serpentine analysed with confocal microscopy after 14 days of perfusion. Dense cellular network covering all surfaces. In blue DAPI, green CD31 and red Phalloidin. B) Part of a channel in detail. C) Orthogonal projection in the XZ axes: complete lumen contained between the endothelial walls. Scalebar 200 µm.*

Chapter 4
CONCLUSIONS

The work done in this thesis was the design and bioprinting of a 3D structure to produce a cell-laden vascularized construct. In recent years, 3D culture has become increasingly important as an improved mimic of the *in vivo* physiological environment. Next to the many advantages this brings, there are also disadvantages: the thicker the structure, the more difficult it becomes to transport nutrients homogeneously throughout; hence the need to create a vascular channel that can be continuously perfused with culture medium, capable of efficiently and uniformly delivering nutrients to cells while also removing waste.

The design of the printed structure, a serpentine contained inside a parallelepiped, was achieved through specific programs such as AutoCAD and PrusaSlicer. Similarly, an *ad hoc* clamp was also designed. This allows printing to be performed directly inside it, and thanks to a PDMS (polydimethylsiloxane) cover, the printed structure is isolated, guaranteeing its sterility. Another advantage given by the clamp is that it has special side holes that allow the insertion of the perfusion nozzles: in this way we know for sure that the needles will enter in the proper part of the serpentine used for inlet and outlet, respectively. This allows the entire structure to be easily moved and perfused for several days without the risk of the needles shifting and causing medium leakage.

Printing and vascularization in 3D were achieved by exploiting a special technique called sacrificial bioprinting, which consents the creation of three-dimensional structures with embedded empty channels. The void channels are obtained exploiting the thermoreversibility of Pluronic®: at room temperature it behaves as a viscous gel, while at temperatures below 10°C it is a liquid. Once the whole structure is obtained and placed in the refrigerator, a wash-out of Pluronic® can be performed to obtain the hollow serpentine. Again, exploiting the concept of thermoreversibility, this time opposite to that seen for the Pluronic®, we chose to use a specific hydrogel to perform the printing of the bulk of the material surrounding the channel. Gelatin methacrylate (GelMA) was the choice because of its characteristics of excellent printability, biocompatibility, non-toxicity, and its in-depth study in the lab. GelMA at 37°C looks like a liquid, while at temperatures below 25°C it is a viscous gel. Having opposite behavior to that of the sacrificial

material, there is no risk of the whole structure dissolving while refrigerating. The concentration of the two hydrogels was studied previously in the laboratory, and an 8% (w/v) for GelMA and 40% (w/v) for Pluronic® was chosen.
Several tests were performed to evaluate the correct printing temperature for GelMA, the correct infill of the structure, and the appropriate printing pressure for Pluronic®. The results led us to choose a GelMA printing temperature of 23.5°C±1 with 80% infill, while a pressure of 410 kPa was chosen for the serpentine printing. All tests were done using a 25G metal-tip needle for both hydrogels.
Once the bioprinting process was optimized, the focus shifted to the biological validation of the structure. First, cell viability and sprout length tests were done on the cell lines used, HUVEC (human umbilical vein endothelial cells) and MSC (mesenchymal stem cells). We chose to use both lines in co-culture because mesenchymal stem cells combined with endothelial cells can stimulate angiogenesis, new vessel formation, and promote the endothelialization process. HUVEC and MSC embedded in GelMA were analyzed after 2, 7 and 14 days of static culture in 50% HUVEC - 50% MSC medium and 100% HUVEC medium. There were no significant differences between the two media formulations, demonstrating that in both environments the cells are viable and properly proliferate over time. Further analysis was done to evaluate how the difference in nutrients provided affects the mesenchymal-to-endothelial transition: the results showed that in samples cultured with HUVEC medium only, the differentiation of MSCs towards an endothelial phenotype is qualitatively stimulated.
The final biological tests focused on the main goal of the thesis, which was to create a construct that can mimic the behavior of a blood vessel, more specifically a capillary. The optimization of the endothelialization protocol was the most difficult step as there are many aspects that lead to the success of the experiment. To obtain the results shown in Chapter 3, the seeding protocol inside the channel has been varied several times to identify the best one. Best results were obtained by seeding with a cell density of 10 million cells per mL of medium in proportion 70% HUVEC and 30% MSC, flipping the structure every 30 minutes for 4 hours to avoid cells deposition by gravity, and leaving the structure in the incubator overnight before connecting it to the perfusion circuit. The circuit consists of a peristaltic pump capable of making flow continuously at a flowrate of 10µL for the first day, then increased to 15µL for subsequent days. In addition, a new type of

reservoir was used: to ensure sterility, two filters are connected to the hoses acting as inlet and outlet, while a third filter is used for air.
The results obtained with this protocol were promising, allowing us to perfuse the entire structure for 14 days and obtain a compact endothelial network and a fully formed lumen.
In the future, more tests will be performed, trying to perfuse the entire structure for as long as possible to consolidate and thicken the endothelial wall. It will then be interesting to perform this type of experiment with the same embedded cells also in GelMA to evaluate the formation of new vessels (angiogenesis) in the 3D construct. In addition, other experiments can be performed by endothelializing the vascular channel in a structure in which tumor cells, like SKNAS (Neuroblastoma tumor cells), are contained in the matrix. The integration of this protocol with cell cultures in the matrix around the channel enable the study of more complex systems, with the aim to properly recreate *in vitro* a vascularized cancer niche, and eventually proceeding with drug testing.

APPENDIX A

In this appendix, some topics related to the characterization of methacrylate gelatin (GelMA), the degree of functionalization chosen, and porosity will be explored. Some protocols related to the steps of endothelialization and immunofluorescence will then be expanded comprehensively.

A.1 GelMA CHARACTERIZATION TESTS

This section reports the results for the GelMA characterization tests previously performed in the laboratory. The results are indicative only of the 8% hydrogel as that is the chosen concentration for the development of this thesis project. Analyses of Nuclear Magnetic Resonance (NMR) spectroscopy are reported. NMR is an instrumental analytical technique that allows detailed information on the structure of molecules to be obtained by observing the behaviour of atomic nuclei in a magnetic field. This makes possible to identify the degree of functionalization (DoF) of GelMA that has been synthesized. As visible in Figure A.1.1, the spectrum shows that the degree of functionalization of GelMA is 70%, as was desired by the synthesis protocol followed. Figure A.1.2 shows an image obtained by Scanning Electron Microscopy (SEM), which allows to assess the pore size of the material under investigation. For the 8% GelMA it was estimated that the pore size is mainly in the range between 10-20 μm, with an average radius of 11.34 μm.

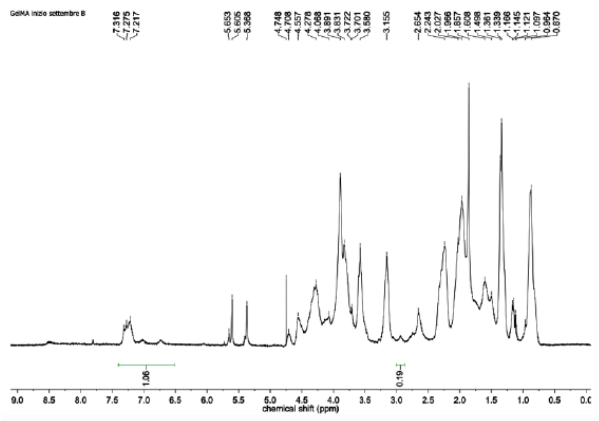

Figure A.1.1*: H-NMR to determine GelMA polymer degree of functionalization (DoF).*

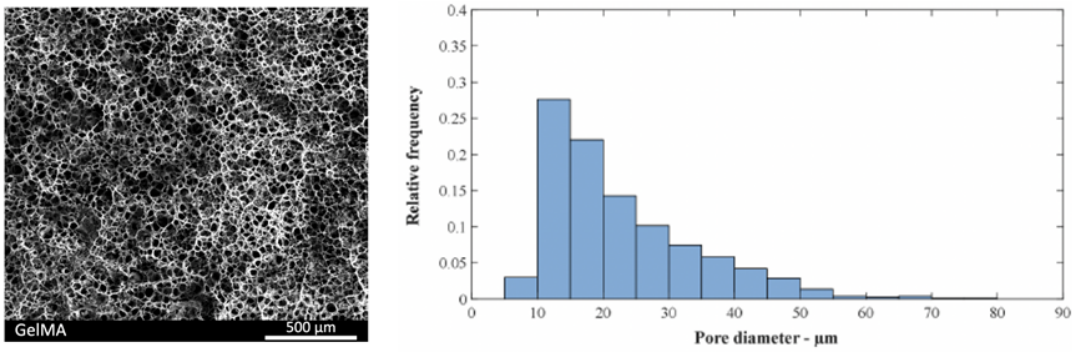

Figure A.1.2*: Scanning Electron Microscopy (SEM). For the 8% GelMA pore size is in the range between 10-20 µm, with an average radius of 11.34 µm.*

A.2 BIOLOGICAL TESTS

This section contains the complete and detailed protocols used to perform the biological tests, particularly the endothelialization protocol and the immunofluorescence protocol using antibodies. Additional images regarding the results obtained for experiments involving prolonged perfusion will be included.

A.2.1 ENDOTHELIALIZATION PROTOCOL

Protocol for the endothelialization part underwent many variations regarding the cell density to be used, the ratio of the two chosen cell lines, and the flipping and resting time before connecting the whole structure to the circuit. Below is the optimized protocol that allowed us to achieve the best results. It is important to underline that all of these steps must be performed under completely sterile conditions.

- load the previously prepared GelMA into the printing cartridge and set it to cool at 4°C for 6 min;
- meanwhile, load the sterile Pluronic® into the printing cartridge. This step requires speed of execution because this material gels quickly once removed from the fridge and put at room temperature;

- insert the two cartridges into the appropriate printheads and select the structure to print;
- set the correct printer parameters, calibrate the two cartridges, and test the hydrogel printing pressure;
- print the structure inside the clamp;
- cross-link using UV light for 1 minute;
- close the print with PDMS and close the entire clamp with screws;
- place the clamp at 4°C for 5 min;
- use two needles to remove liquid Pluronic® by injecting cold 1xPBS inside the channel;
- seed the cells (70% HUVEC - 30% MSC) inside the channel at a density of 10 million cells per mL of medium;
- place the structure in incubator at 37°C. Turn it 180° every 30 minutes for 4 hours;
- gently inject HUVEC medium inside the canal to remove unattached cells and provide new nutrients to the cells present. Leave the structure to rest overnight;
- the next day connect the construct to the perfusion circuit consisting of: peristaltic pump, reservoir containing 60 mL of HUVEC medium only, hoses and syringe filters. Set the speed to 0.5 rpm (10 µL) for the first day and in subsequent days raise it to 0.7 rpm (15 µL);
- keep the structure and reservoir in incubator at 37°C.

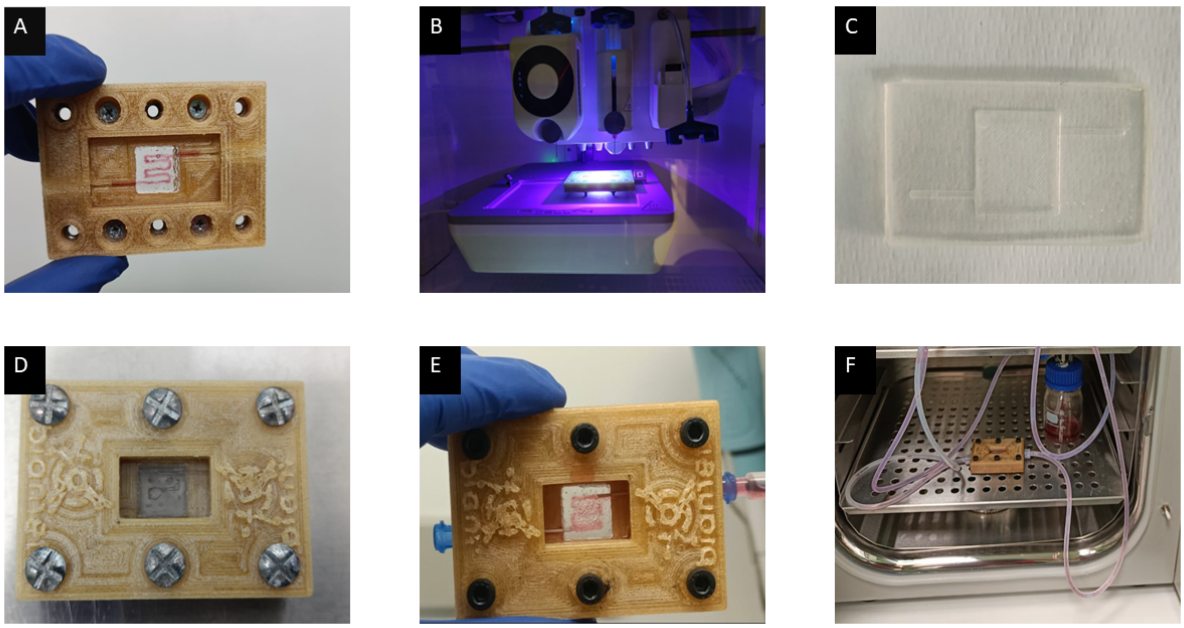

Figure A.2.1: *illustrative photos of key steps in the endothelialization protocol (performed under nonsterile conditions). A) printing of the structure inside the clamp; B) cross-linking with UV light for one minute; C) PDMS cover; D) clamp after 5 minutes at 4°C; E) wash-out of Pluronic® with cold 1xPBS; F) after seeding cells, flipping for 4 hours and having left overnight, connecting the structure to the reservoir; all inside the incubator at 37°C.*

A.2.2 IMMUNOFLUORESCENCE PROTOCOL

This protocol has also undergone several changes. In fact, because of the thickness of the bioprinted structure, with the initial protocol the antibodies struggled to bind targets even in the most internal areas of the construct. The protocol reported here is the one that gave us the best results.

- detach the perfusion circuit;
- remove the printed structure from the clamp and do washes with 1xPBS inside multiwell plates;
- place the structure in a well containing 4% w/v paraformaldehyde (PFA) for 4 hours at 4°C. Suggestion: after two hours, cut the sample in half to allow the solution to enter deeply;
- perform washes with PBS-T (1xPBS with 0.1% w/v Tryton X-100);

- immerge the structure in Blocking Solution (BS = BSA 1% w/v + Tryton X-100 0.1% w/v) for 4 hours at room temperature;
- do some washes with PBS-T;
- place the structure in a well containing primary antibodies diluted in Blocking Solution. Refrigerate at 4°C for a day;
- soak the structure in PBS-T + BSA 0.5% w/v and leave it overnight at 4°C;
- put the structure in a solution of BS + secondary antibodies and leave at room temperature for 8 hours;
- perform washes with PBS-T;
- leave the structure immersed in PBS-T + BSA 0.5% w/v in fridge overnight;
- next morning add other dyes if desired (like DAPI and phalloidin);
- wash with 1xPBS to remove unbound molecules.

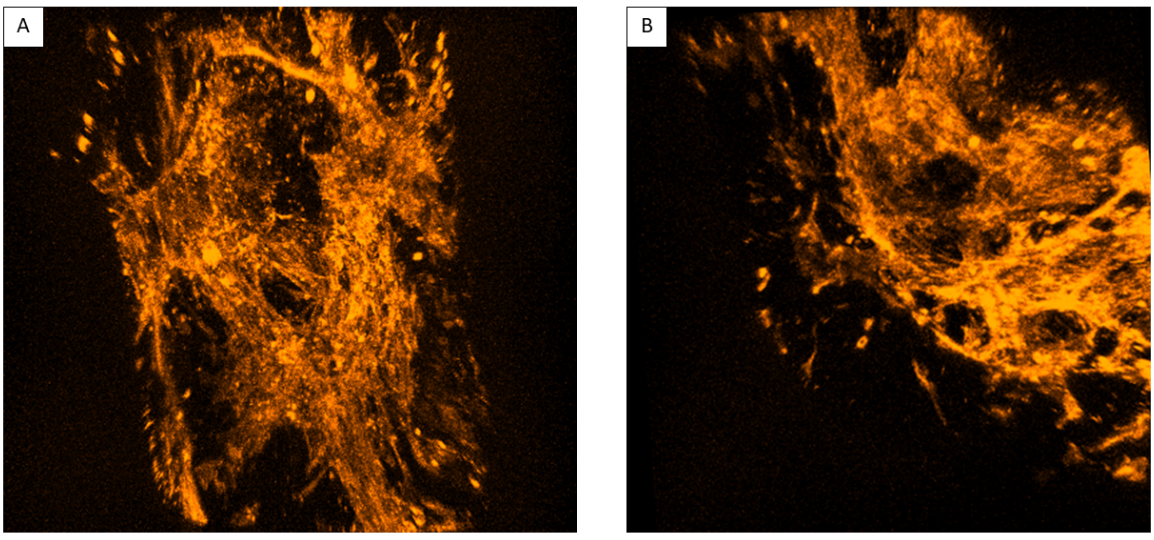

Figure A.2.2: *immunofluorescence analysis on endothelialized channel (HUVEC 70% + MSC 30%, cell density $10 \cdot 10^6$ cells/mL) perfused for 7 days. A) Linear channel; B) corner of channel.*

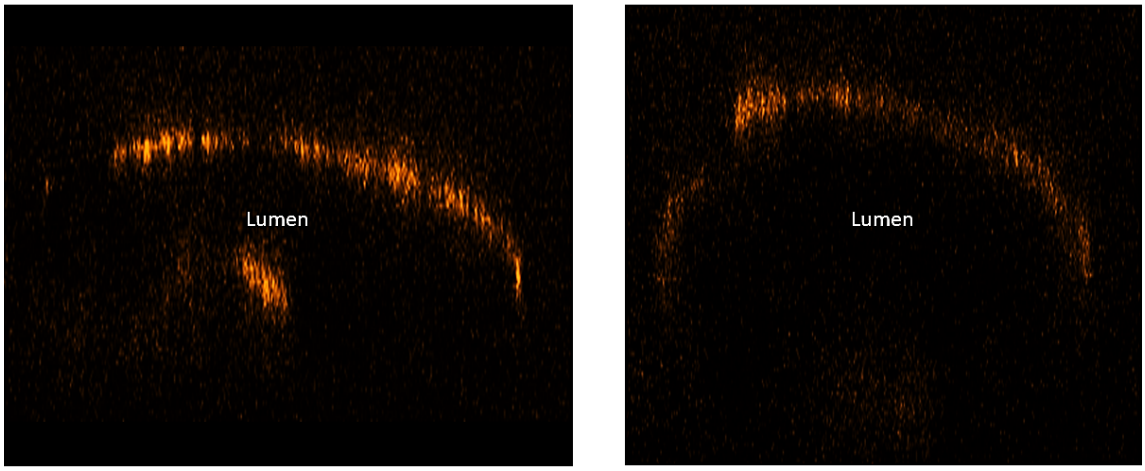

Figure A.2.3: *lumens of two different sections of the endothelialized channel (HUVEC 70% + MSC 30%, cell density $10 \cdot 10^6$ cells/mL) perfused for 7 days. As visible, the lumen is not fully formed.*

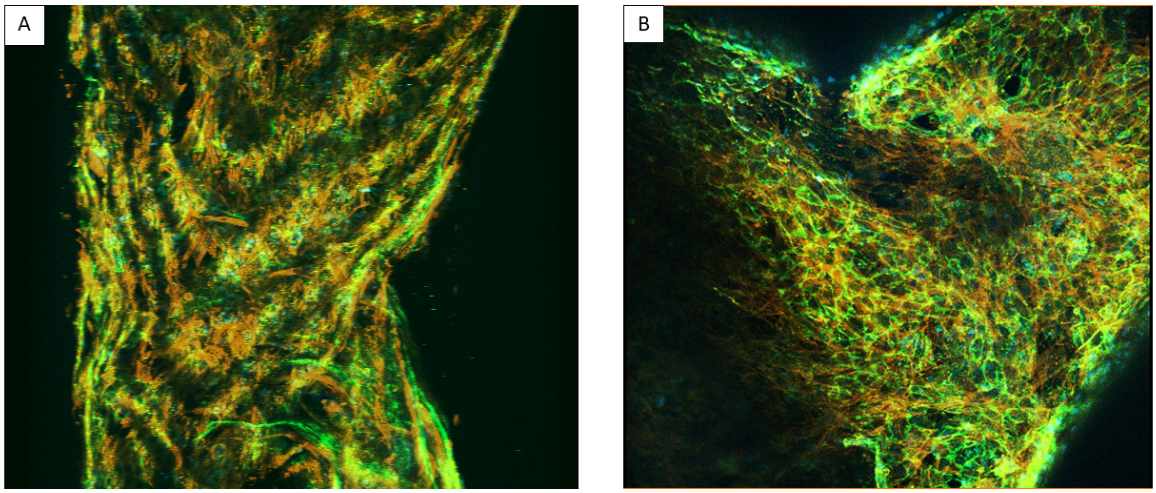

Figure A.2.4: *immunofluorescence analysis on endothelialized channel (HUVEC 70% + MSC 30%, cell density $10 \cdot 10^6$ cells/mL) perfused for 14 days. A) Linear channel; B) corner of channel.*

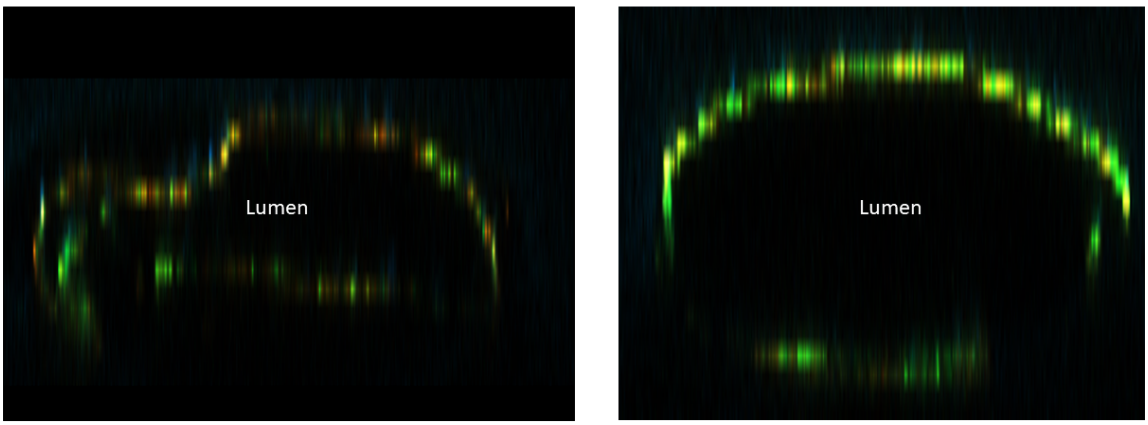

Figure A.2.5: *lumens of two different sections of the endothelialized channel (HUVEC 70% + MSC 30%, cell density $10 \cdot 10^6$ cells/mL) perfused for 14 days. As visible, the lumen is completely formed.*

BIBLIOGRAPHY

[1] Kayla Duval, Hannah Grover, Li-Hsin Han, Yongchao Mou, Adrian F. Pegoraro, Jeffery Fredberg, Zi Chen. *Modeling physiological events in 2d vs.3d cell culture.* PHYSIOLOGY 32: 266–277, 2017. https://doi.org/10.1152/physiol.00036.2016

[2] Rajat K. Das, Omar F. Zouani*. A review of the effects of the cell environment physicochemical nanoarchitecture on stem cell commitment.* Biomaterials, Volume 35, Issue 20, 2014, Pages 5278-5293, ISSN 0142-9612, https://doi.org/10.1016/j.biomaterials.2014.03.044

[3] Francesco Rosso, Antonio Giordano, Manlio Barbarisi, Alfonso Barbarisi. *From cell–ECM interactions to tissue engineering.* Journal of cellular physiology 199:174–180(2004). https://doi.org/10.1002/jcp.10471

[4] McKee, T.J., Perlman, G., Morris, M. et al. *Extracellular matrix composition of connective tissues: a systematic review and meta-analysis*. Scientific Report 9, 10542 (2019). https://doi.org/10.1038/s41598-019-46896-0

[5] Sjoerd van Helvert, Cornelis Storm and Peter Friedl. *Mechanoreciprocity in cell migration*. Nature Cell Biology 20, 8–20 (2018). https://doi.org/10.1038/s41556-017-0012-0

[6] Yu Zheng, Hanqing Nan, Yanping Liu, Qihui Fan, Xiaochen Wang, Ruchuan Liu, Liyu Liu, Fangfu Ye, Bo Sun, and Yang Jiao. *Modeling cell migration regulated by cell extracellular-matrix micromechanical coupling*. Physical Review E 100, 043303 (2019). https://doi.org/10.1103/PhysRevE.100.043303

[7] Marco Cantini, Hannah Donnelly, Matthew J. Dalby, Manuel Salmeron-Sanchez. *The plot thickens: the emerging role of matrix viscosity in cell mechanotransduction*. Advanced Healthcare Material 2020, 9, 1901259 https://doi.org/10.1002/adhm.201901259

[8] Delphine Antoni, Hélène Burckel, Elodie Josset and Georges Noel. *Three-dimensional cell culture: a breakthrough in vivo*. International Journal of Molecular Sciences 2015, 16(3), 5517-5527. https://doi.org/10.3390/ijms16035517

[9] Rasheena Edmondson, Jessica Jenkins Broglie, Audrey F. Adcock, and Liju Yang. *Three-dimensional cell culture systems and their applications in drug discovery and cell-based biosensors*. ASSAY and Drug Development Technologies 2014. Volume: 12, Issue 4: 207- 218. https://doi.org/10.1089/adt.2014.573

[10] Marta Kapałczyńska, Tomasz Kolenda, Weronika Przybyła, Maria Zajączkowska, Anna Teresiak, Violetta Filas, Matthew Ibbs, Renata Bliźniak, Łukasz Łuczewski, Katarzyna Lamperska. *2D and 3D cell cultures–a comparison of different types of cancer cell cultures*. Archives of Medical Science, 2018, 14.4: 910-919. https://doi.org/10.5114/aoms.2016.63743

[11] Jensen Caleb and Teng Yong. *Is It Time to Start Transitioning From 2D to 3D Cell Culture?* Frontiers in Molecular Biosciences 2020, Volume 7. ISSN: 2296-889X. https://doi.org/10.3389/fmolb.2020.00033

[12] Steven R Caliari, Jason A Burdick. *A practical guide to hydrogels for cell culture*. Nature Methods 13, 405–414 (2016). https://doi.org/10.1038/nmeth.3839

[13] Yi Zhang, Piyush Kumar, Songwei Lv, Di Xiong, Hongbin Zhao, Zhiqiang Cai, Xiubo Zhao. *Recent advances in 3D bioprinting of vascularized tissues*. Materials & Design, Volume 199, 2021, 109398, ISSN 0264-1275, https://doi.org/10.1016/j.matdes.2020.109398

[14] Ying Huang, Xiao-Fei Zhang, Guifang Gao, Tomo Yonezawa, Xiaofeng Cui. *3D bioprinting and the current applications in tissue engineering*. Biotechnology Journal 2017, 12, 1600734. doi:10.1002/biot.201600734

[15] Jürgen Groll et al. *Biofabrication: reappraising the definition of an evolving field*. Biofabrication, 8 (2016) 013001. doi:10.1088/1758-090/8/1/013001

[16] Gregory Gillispie et al. *Assessment methodologies for extrusion-based bioink printability*. Biofabrication 12 (2020) 022003. https://doi.org/10.1088/1758-5090/ab6f0d

[17] Chaoran Dou, Victoria Perez, Jie Qu, Andrew Tsin, Ben Xu, Jianzhi Li. *A state-of-the-art review of laser-assisted bioprinting and its future research trends*. ChemBioEng Reviews 2021,8, No. 5, 517–534. https://doi.org/10.1002/cben.202000037

[18] Bagrat Grigoryan, Daniel W. Sazer, Amanda Avila, Jacob L. Albritton, Aparna Padhye, Anderson H. Ta, Paul T. Greenfield, Don L. Gibbons and Jordan S. Miller. *Development, characterization, and applications of multi-material stereolithography bioprinting*. Scientific Reports 11, 3171 (2021). https://doi.org/10.1038/s41598-021-82102-w

[19] Swati Midha, Manu Dalela, Deborah Sybil, Prabir Patra, Sujata Mohanty. *Advances in three-dimensional bioprinting of bone: Progressand challenges*. Journal of Tissue Engineering and Regenerative Medicine, Volume13, Issue6, June 2019, Pages 925-945. https://doi.org/10.1002/term.2847

[20] Cui, Xiaofeng; Boland, Thomas; D.D'Lima, Darryl; K. Lotz, Martin. *Thermal Inkjet Printing in Tissue Engineering and Regenerative Medicine*. Recent Patents on Drug Delivery & Formulation, Volume 6, Number 2, 2012, pp. 149-155(7). https://doi.org/10.2174/187221112800672949

[21] Nhayoung Hong, Gi-Hoon Yang, JaeHwan Lee, GeunHyung Kim. *3D bioprinting and its in vivo applications.* Journal of biomedical materials research. Volume 106, Issue 1, 2018, pages: 444-459. https://doi.org/10.1002/jbm.b.33826

[22] Christian Mandrycky, Zongjie Wang, Keekyoung Kim, Deok-Ho Kim. *3D bioprinting for engineering complex tissues*. Biotechnology Advances, Volume 34, Issue 4, 2016, pages 422-434, ISSN 0734-9750. https://doi.org/10.1016/j.biotechadv.2015.12.011

[23] Ashkan Shafiee, Anthony Atala. P*rinting technologies for medical applications*. Trends in Molecular Medicine, Volume 22, Issue 3, 2016, pages 254-265. https://doi.org/10.1016/j.molmed.2016.01.003

[24] Enas M. Ahmed. *Hydrogel: Preparation, characterization, and applications: A review*. Journal of Advanced Research, Volume 6, Issue 2, 2015, pages 105-121, ISSN 2090-1232, https://doi.org/10.1016/j.jare.2013.07.006

[25] K. Pal, A. K. Banthia, D. K. Majumdar. *Polymeric hydrogels: characterization and biomedical applications*. Designed Monomers and Polymers, 12:3, 197-220 (2019). https://doi.org/10.1163/156855509X436030

[26] Desireé Alesa Gyles, Lorena Diniz Castro, José Otávio Carréra Silva, Roseane Maria Ribeiro-Costa. *A review of the designs and prominent biomedical advances of natural and synthetic hydrogel formulations*. European Polymer Journal, Volume 88, 2017, Pages 373-392, ISSN 0014-3057. https://doi.org/10.1016/j.eurpolymj.2017.01.027

[27] Sweta Garg, Ashish Garg. *Hydrogel: classification, properties, preparation and technical features*. Asian Journal of Biomaterial Research 2016; 2(6): 163-170.

[28] Faheem Ullah, Muhammad Bisyrul Hafi Othman, Fatima Javed, Zulkifli Ahmad, Hazizan Md. Akil. *Classification, processing and application of hydrogels: a review*. Materials Science and Engineering: C, Volume 57, 2015, pages 414-433. https://doi.org/10.1016/j.msec.2015.07.053

[29] Swati Sharma, Shachi Tiwari. *A review on biomacromolecular hydrogel classification and its applications*. International Journal of Biological Macromolecules, Volume 162, 2020, Pages 737-747, ISSN 0141-8130, https://doi.org/10.1016/j.ijbiomac.2020.06.110

[30] Jeon Il Kanga, Kyung Min Park. *Advances in gelatin-based hydrogels for wound management*. Journal of Materials Chemistry B, 2021, 9, 1503-1520. https://doi.org/10.1039/D0TB02582H

[31] Wang, Xiaohong, Qiang Ao, Xiaohong Tian, Jun Fan, Hao Tong, Weijian Hou, and Shuling Bai. *Gelatin-Based Hydrogels for Organ 3D Bioprinting*. Polymers 9, 2017, no. 9: 401. https://doi.org/10.3390/polym9090401

[32] Jing Ye, Zhenghua Xiao, Lu Gao, Jing Zhang, Ling He, Han Zhang, Qi Liu and Gang Yang. *Assessment of the effects of four crosslinking agents on gelatin hydrogel for myocardial tissue engineering applications*. Biomedical Material 16 045026. https://doi.org/10.1088/1748-605X/abfff2

[33] Juthamas Ratanavaraporn, Ratthapol Rangkupan, Hathairat Jeeratawatchai, Sorada Kanokpanont, Siriporn Damrongsakkul. *Influences of physical and chemical crosslinking techniques on electrospun type A and B gelatin fiber mats*. International Journal of Biological Macromolecules, Volume 47, Issue 4, 2010, pages 431-438, ISSN 0141-8130. https://doi.org/10.1016/j.ijbiomac.2010.06.008

[34] Liu Taotao, Wenxian Weng, Yuzhuo Zhang, Xiaoting Sun, and Huazhe Yang. *Applications of Gelatin Methacryloyl (GelMA) Hydrogels in Microfluidic Technique-Assisted Tissue Engineering*. Molecules 25, 2020, no. 22: 5305. https://doi.org/10.3390/molecules25225305

[35] Kan Yue, Grissel Trujillo-de Santiago, Mario Moisés Alvarez, Ali Tamayol, Nasim Annabi, Ali Khademhosseini. *Synthesis, properties, and biomedical applications of gelatin methacryloyl (GelMA) hydrogels*. Biomaterials, Volume 73, 2015, pages 254-271, ISSN 0142-9612. https://doi.org/10.1016/j.biomaterials.2015.08.045

[36] Jason W. Nichol, Sandeep T. Koshy, Hojae Bae, Chang M. Hwang, Seda Yamanlar, Ali Khademhosseini. *Cell-laden microengineered gelatin methacrylate hydrogels*. Biomaterials, Volume 31, Issue 21, 2010, pages 5536-5544. https://doi.org/10.1016/j.biomaterials.2010.03.064

[37] Michael Müller, Jana Becher, Matthias Schnabelrauch, Marcy Zenobi-Wong. *Nanostructured pluronic hydrogels as bioinks for 3D bioprinting*. Biofabrication, Volume 7, Number 3, 035006, 2015. doi:10.1088/1758-5090/7/3/035006

[38] Emilia Gioffredi, Monica Boffito, Stefano Calzone, Sara Maria Giannitelli, Alberto Rainer, Marcella Trombetta, Pamela Mozetic, Valeria Chiono. *Pluronic F127 hydrogel characterization and biofabrication in cellularized constructs for tissue engineering applications*. Procedia CIRP, Volume 49, 2016, pages 125-132. https://doi.org/10.1016/j.procir.2015.11.001

[39] Miller J., Stevens K., Yang M. et al. *Rapid casting of patterned vascular networks for perfusable engineered three-dimensional tissues*. Nature Mater 11, 768–774 (2012). https://doi.org/10.1038/nmat3357

[40] Richards D., Jia J., Yost M. et al. *3D bioprinting for vascularized tissue fabrication*. Annals of Biomedical Engineering 45, 132–147 (2017). https://doi.org/10.1007/s10439-016-1653-z

[41] Amir K. Miri, Akbar Khalilpour, Berivan Cecen, Sushila Maharjan, Su Ryon Shin, Ali Khademhossein. *Multiscale bioprinting of vascularized models*. Biomaterials, Volume 198, 2019, pages 204-216, ISSN 0142-9612, https://doi.org/10.1016/j.biomaterials.2018.08.006

[42] Liu Siyu, Tianlin Wang, Shenglong Li, Xiaohong Wang. A*pplication status of sacrificial biomaterials in 3D bioprinting*. Polymers 14, 2022, no. 11: 2182. https://doi.org/10.3390/polym14112182

[43] David Koleskya, Kimberly Homana, Mark Skylar-Scotta, Jennifer Lewisa. *Three-dimensional bioprinting of thick vascularized tissues*. PNAS 2016, vol. 113, no. 12, pages:3179–3184. https://doi.org/10.1073/pnas.1521342113

[44] Ruoxiao Xie, Wenchen Zheng, Liandi Guan, Yongjian Ai, and Qionglin Liang. *Engineering of hydrogel materials with perfusable microchannels for building vascularized tissues*. Small 2020, Volume 16, Issue 15, 1902838. https://doi.org/10.1002/smll.201902838

[45] Wen Jie Zhang, Wei Liu, Lei Cui, Yilin Cao. *Tissue engineering of blood vessel*. Journal of Cellular and Molecular Medicine, Volume 11, Issue 5, pages: 945-957, 2007. doi.org/10.1111/j.1582-4934.2007.00099.x

[46] Liliang Ouyang, James P. K. Armstrong, Qu Chen, Yiyang Lin, and Molly M. Stevens. *Void-free 3D bioprinting for in situ endothelialization and microfluidic perfusion*. Advanced Functional Materials 2020, Volume 30, Issue 1, 1908349. https://doi.org/10.1002/adfm.201908349

[47] Shirahama H, Lee B, Tan L. et al. *Precise Tuning of Facile One-Pot Gelatin Methacryloyl (GelMA) Synthesis*. Sci Rep 6, 31036 (2016). https://doi.org/10.1038/srep31036

[48] Medina-Leyte, Diana J., Mayra Domínguez-Pérez, Ingrid Mercado, María T. Villarreal-Molina, and Leonor Jacobo-Albavera*. Use of Human Umbilical Vein Endothelial Cells (HUVEC) as a Model to Study Cardiovascular Disease: A Review*. Applied Sciences 10, no. 3: 938 (2020) https://doi.org/10.3390/app10030938

[49] Katarina Le Blanc, Lindsay C. Davies. *MSCs—cells with many sides*. Cytotherapy, Volume 20, Issue 3, 2018, Pages 273-278, ISSN 1465-3249, https://doi.org/10.1016/j.jcyt.2018.01.009

[50] Nicholas Law, Brandon Doney, Hayley Glover, Yahua Qin, Zachary M. Aman, Timothy B. Sercombe, Lawrence J. Liew, Rodney J. Dilley, Barry J. Doyle. *Characterisation of hyaluronic acid methylcellulose hydrogels for 3D bioprinting.* Journal of the Mechanical Behavior of Biomedical Materials, Volume 77, 2018, Pages 389-399, ISSN 1751-6161. https://doi.org/10.1016/j.jmbbm.2017.09.031

[51] Sílvia J. Bidarra, Cristina C. Barrias, Mário A. Barbosa, Raquel Soares, Joelle Amédée, Pedro L. Granja. *Phenotypic and proliferative modulation of human mesenchymal stem cells via crosstalk with endothelial cells*. Stem Cell Research, Volume 7, Issue 3, 2011, Pages 186-197, ISSN 1873-5061, https://doi.org/10.1016/j.scr.2011.05.006

[52] Carpentier G., Berndt S., Ferratge S. et al. *Angiogenesis Analyzer for ImageJ — A comparative morphometric analysis of "Endothelial Tube Formation Assay" and "Fibrin Bead Assay"*. Scientific Report 10, 11568 (2020). https://doi.org/10.1038/s41598-020-67289-8